AEDC-TR-69-58

TEMPERATURE DEVELOPMENT IN THE ENTRANCE REGION OF A PARALLEL PLATE CHANNEL WITH WALL BLOWING

James R. Blanks

ARO, Inc.

May 1969

VON KÁRMÁN GAS DYNAMICS FACILITY
ARNOLD ENGINEERING DEVELOPMENT CENTER
AIR FORCE SYSTEMS COMMAND
ARNOLD AIR FORCE STATION, TENNESSEE

NOTICES

When U. S. Government drawings specifications, or other data are used for any purpose other than a definitely related Government procurement operation, the Government thereby incurs no responsibility nor any obligation whatsoever, and the fact that the Government may have formulated, furnished, or in any way supplied the said drawings, specifications, or other data, is not to be regarded by implication or otherwise, or in any manner licensing the holder or any other person or corporation, or conveying any rights or permission to manufacture, use, or sell any patented invention that may in any way be related thereto.

Qualified users may obtain copies of this report from the Defense Documentation Center.

References to named commercial products in this report are not to be considered in any sense as an endorsement of the product by the United States Air Force or the Government.

TEMPERATURE DEVELOPMENT IN THE ENTRANCE REGION OF A PARALLEL PLATE CHANNEL WITH WALL BLOWING

James R. Blanks
ARO, Inc.

FOREWORD

The research reported herein was sponsored by Headquarters, Arnold Engineering Development Center (AEDC), Air Force Systems Command (AFSC), Arnold Air Force Station, Tennessee, under Program Element 65401F, Project 876A, Task G226.

The results of research were obtained by ARO, Inc. (a subsidiary of Sverdrup & Parcel and Associates, Inc.), contract operator of AEDC, AFSC, under Contract F40600-69-C-0001. The research was performed from December 1967 to April 1968 under ARO Project No. VT8002, and the manuscript was submitted for publication on February 13, 1969.

The work reported herein was used as a thesis for partial fulfillment of the requirements for the degree of Master of Science from The University of Tennessee Space Institute. The author wishes to express his appreciation to Dr. Arsev H. Eraslan, Associate Professor of Aerospace Engineering at The University of Tennessee Space Institute, for his direction throughout the course of this investigation.

This technical report has been reviewed and is approved.

Eugene C. Fletcher
Lt Colonel, USAF
AF Representative, VKF
Directorate of Test

Roy R. Croy, Jr.
Colonel, USAF
Director of Test

ABSTRACT

The general mathematical problem of the thermal entrance region is formulated for a parallel plate channel by including the effects of viscous dissipation, axial conduction, and wall blowing. The associated eigenvalue problem is solved by the B. G. Galerkin method and the results are presented for constant wall temperature. It is shown that the particular method has distinct computational advantages over the classical form of solutions. The constant wall temperature case is investigated by employing the solutions of the eigenvalue problem, and it is concluded that the wall blowing parameter has considerable effect on the temperature development. The axial conduction term is also shown to have considerable effect on the temperature development for low values of Peclet number.

CONTENTS

ILLUSTRATIONS

TABLES

NOMENCLATURE

A_n	Constant defined by Equation 43
C_p	Specific heat at constant pressure
Ec	Pseudo-Eckert number defined by Equation 16
F_n	Modified eigenfunction defined by Equation 29
L	Channel width
$Nu^{(0)}$	Nusselt number defined by Equation 63
$Nu^{(1)}$	Nusselt number defined by Equation 64
$\overline{Nu}$	Average Nusselt number defined by Equation 75
P	Pressure
Pe	Peclet number defined by Equation 16
Pr	Prandtl number defined by Equation 16
Q	Net heat transfer defined by Equation 74
R_c	Characteristic Reynolds number defined by Equation 16
T	Dimensional temperature
T_m	Bulk mean temperature defined by Equation 59
T_o^*	Characteristic entrance temperature
u	Non-dimensional velocity component defined by Equation 12
V	Velocity component shown in Figure 1
V_c	Characteristic velocity defined by Equation 11
x	Space coordinate shown in Figure 1
y	Non-dimensional space coordinate
z	Non-dimensional space coordinate defined by Equation 12

β_n	Eigenvalues given in Equation 26
θ	Non-dimensional temperature defined by Equation 12
θ_m	Non-dimensional bulk temperature defined by Equation 60
Ω	Excess temperature defined by Equation 22
Ω_n	Eigenfunction given in Equation 26
κ	Thermal conductivity
ν	Kinematic viscosity
ξ	Non-dimensional space coordinate defined by Equation 22
ρ	Mass density
λ	Wall velocity parameter defined by Equation 16
Φ	Dissipation function
Ψ	Non-dimensional dissipation function defined by Equation 15
ϕ_k	B. G. Galerkin function set defined by Equation 36

SUBSCRIPTS

w	Wall conditions
o	Entrance conditions
1	Direction indicated in Figure 1
2	Direction indicated in Figure 1
3	Direction indicated in Figure 1
∞	Denotes fully developed conditions

CHAPTER I
INTRODUCTION

The heat transfer in laminar flow of an incompressible, non-viscous fluid in the entrance region of a circular tube was first investigated analytically by Graetz (1)[1], under the assumption of specified uniform wall temperature and fully developed velocity profiles. Prins, Mulder, and Schenk (2) solved the analogous problem with plane parallel plates substituted for the cylindrical tube wall. Various authors (3-8) have extended analysis of the problem by considering increasing complexity of the boundary conditions and velocity distributions for circular tubes and parallel plates.

Abramowitz (9) and Sellars, Tribus, and Klein (10) have presented in detail the classical mathematical solutions of the eigenvalue problem encountered in the analysis of thermal entrance regions. These authors concluded that the evaluation of the eigenvalues and the eigenfunctions from the exact analytical expressions resulted in considerable computational difficulties even in the cases of relatively simple flow and thermal boundary conditions.

Sparrow and Siegel (11) introduced the successful application of variational methods to the mathematical problem for parallel plate channels and finite cross-sectional ducts and approximate solutions

---

[1]Numbers in parentheses refer to similarly numbered references in the bibliography.

were found to be in reasonable agreement with the available exact solutions for certain special cases. Direct numerical solutions for various hydrodynamic velocity profiles in circular tubes were presented by Kays (12) who compared the results for the Graetz problem against the exact solutions.

Hsu (13) presented an exact mathematical solution for the entrance region laminar heat transfer including the effects of axial conduction. The temperature solution for pipe flow corresponding to the boundary condition of uniform wall heat flux was obtained. The corresponding problem in parallel plate geometry was treated by Agrawal (14) for the boundary conditions of constant wall temperature. The eigenfunctions were expanded as an infinite Fourier-sine series, and the temperature solution corresponding to a Peclet number, Pe = 1, based on the mean velocity was obtained. These authors concluded that the effect of axial conduction was significant for low Peclet numbers.

LeCroy (15) investigated the feasibility of application of the B. G. Galerkin method (16) to formulate approximate solutions for the temperature development in parallel plate MHD channel flows by including the effects of viscous dissipation, Joule heating, non-zero net current, and axial heat conduction.

The previously mentioned authors (1-15) investigated the thermal entrance region problem assuming channels and ducts with solid walls.

The purpose of the present study is to develop approximate solutions for the temperature development and local Nusselt number in

parallel plate channel flows with wall blowing by the application of the B. G. Galerkin method (16). The problem was formulated to include the effects of viscous dissipation and axial heat conduction.

CHAPTER II
ANALYTIC PROCEDURE

I. GOVERNING EQUATIONS AND BOUNDARY CONDITIONS

Consider a fluid of constant properties flowing between infinite parallel plates. The mathematical problem is formulated in the Cartesian coordinate system (x_1, x_2, x_3), with x_3 taken at the base of the channel along the direction of the applied pressure gradient, dP/dx_3. The origin of the system is taken at the point of intersection of the x_3 axis with the plane at which the thermal entrance region initiates, as shown in Figure 1. It is assumed that there is a constant injection of fluid through the wall at $x_2 = 0$, and that there is a constant suction of fluid through the wall at $x_2 = L$. The mass flow rate due to injection is assumed to be equal to that due to suction producing a velocity component, V_w. It is further assumed that the flow is fully developed at the thermal entrance plane.

For fully developed flow conditions and for a parallel plate channel configuration of infinite dimensions along x_1 and x_3, with no velocity component along x_i direction, it is concluded that the applied axial pressure gradient, dP/dx_3, is a constant.

The governing equations for fully developed, steady state, incompressible flow of a viscous fluid with constant properties for infinite parallel plates along the x_1 direction are:

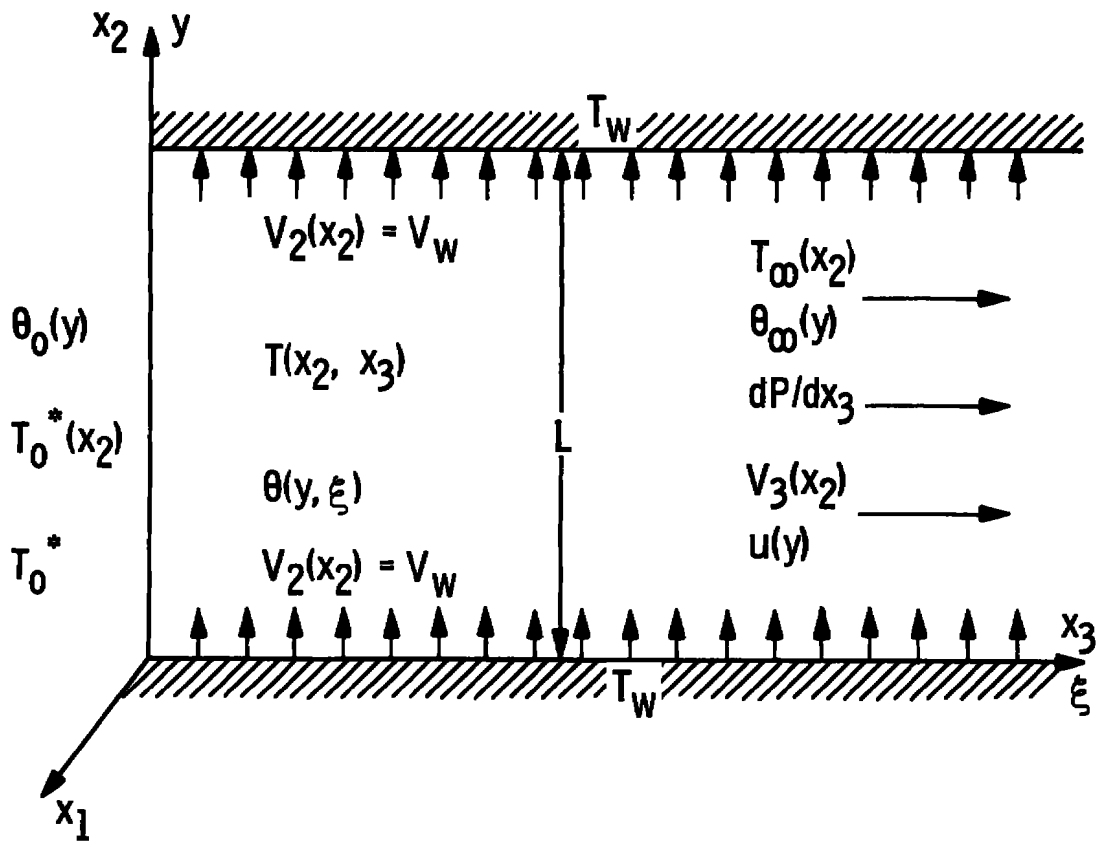

Fig. 1 Channel Geometry

Continuity equation,

$$\frac{\partial V_2}{\partial x_2}(x_2) = 0 \tag{1}$$

which integrates into,

$$V_2(x_2) = V_w = \text{constant} \tag{2}$$

Momentum equation,

$$\nu \frac{\partial^2 V_3}{\partial x_2^2}(x_2) - V_w \frac{\partial V_3}{\partial x_2}(x_2) - \frac{1}{\rho}\frac{\partial P}{\partial x_3} = 0 \tag{3}$$

Energy equation,

$$\rho C_p \left[V_w \frac{\partial T}{\partial x_2}(x_2,x_3) + V_3(x_2) \frac{\partial T}{\partial x_3}(x_2,x_3) \right] =$$

$$\kappa \left[\frac{\partial^2 T}{\partial x_2^2}(x_2,x_3) + \frac{\partial^2 T}{\partial x_3^2}(x_2,x_3) \right] + \Phi(x_2) \tag{4}$$

where the dissipation function, $\Phi(x_2)$, is given by,

$$\Phi(x_2) = \rho\nu \left[\frac{dV_3}{dx_2}(x_2) \right]^2 \tag{5}$$

The hydrodynamic boundary conditions on the velocity component, $V_3(x_2)$, are determined according to the nonslip conditions on the stationary walls,

$$V_3(0) = 0, \quad V_3(L) = 0 \tag{6}$$

The temperature distribution is prescribed at the thermal entrance plane, $x_3 = 0$, as a function of x_2,

$$T(x_2,0) = T_o(x_2) \tag{7}$$

and is prescribed as equal temperatures at both walls of the parallel plate channel,

$$T(0,x_3) = T_w,\ T(L,x_3) = T_w \tag{8}$$

The remaining condition on the temperature distribution is determined from the thermally fully developed condition, $T_\infty(x_2,x_3)$, by solving the limiting case, $x_3 \to \infty$, of the energy equation,

$$k\frac{d^2T_\infty}{dx_2^2}(x_2) - \rho c_p v_w \frac{dT_\infty}{dx_2}(x_2) + \Phi(x_2) = 0 \tag{9}$$

under the boundary conditions,

$$T_\infty(0) = T_w,\ T_\infty(L) = T_w \tag{10}$$

There would be little change in the further mathematical development of the problem if the thermal boundary conditions on the channel walls were assumed to be constant wall temperatures of unequal value.

II. NON-DIMENSIONAL PROBLEM

The mathematical system is non-dimensionalized based on the constant pressure gradient by defining a characteristic velocity, V_c, as

$$V_c = - \frac{L^2}{\rho\nu} \frac{dP}{dx_3} \tag{11}$$

with the following dimensionless variables and parameters:

$$y = \frac{x_2}{L} , \quad z = \frac{x_3}{L} , \quad u(y) = \frac{V_3(x_2)}{V_c} ,$$

$$\theta = \frac{T(x_2,x_3) - T_w}{T_o^* - T_w} , \quad \theta_o = \frac{T_o - T_w}{T_o^* - T_w} ,$$

$$\Psi(y) = \frac{L^2}{K(T_o^* - T_w)} \Phi(x_2) \tag{12}$$

where T_o^* is a characteristic value associated with the entrance temperature distribution, $T_o(x_2)$.

The dimensionless forms of the momentum equation, Equation 3, and the energy equation, Equation 4, respectively, become

$$\frac{d^2u}{dy^2}(y) - R_c\lambda \frac{du}{dy}(y) = - 1 \tag{13}$$

$$Pe\left[u(y) \frac{\partial\theta}{\partial z}(y,z) + \lambda \frac{\partial\theta}{\partial y}(y,z)\right] = \frac{\partial^2\theta}{\partial y^2}(y,z) + \frac{\partial^2\theta}{\partial z^2}(y,z) + \Psi(y) \tag{14}$$

where the dimensionless dissipation function is

$$\Psi(y) = Pr\ Ec \left[\frac{du}{dy}(y)\right]^2 \tag{15}$$

In Equations 13 through 15 the dimensionless parameters are defined as:

$$Ec = \frac{V_c^2}{C_p(T_o^* - T_w)} = \text{Pseudo. Eckert Number}$$

$$Pe = \frac{\rho V_c C_p L}{\kappa} = \text{Peclet Number}$$

$$Pr = \frac{C_p \rho \nu}{\kappa} = \text{Prandtl Number}$$

$$\lambda = \frac{V_w}{V_c} = \text{Wall Velocity Parameter}$$

$$Rc = \frac{V_c L}{\nu} = \text{Characteristic Reynolds Number}$$

$$Rc\lambda = \frac{V_w L}{\nu} = \text{Wall Blowing Parameter} \qquad (16)$$

The boundary condition for the dimensionless velocity u(y), becomes

$$u(0) = 0, \; u(1) = 0 \qquad (17)$$

and the thermal boundary conditions for the dimensionless temperature, $\theta(y,z)$, at the thermal entrance, and at the walls are:

$$\theta(y,0) = \theta_o(y), \quad \theta(0,z) = 0, \quad \theta(L,z) = 0 \qquad (18)$$

The remaining boundary condition required to complete the solution is determined from the thermally fully developed dimensionless temperature distribution, $\theta_\infty(y)$,

$$\theta_\infty(y) = \lim_{z \to \infty} \theta(y,z) \qquad (19)$$

Solving the limiting case, $z \to \infty$, of the non-dimensional energy equation, Equation 14, the mathematical system becomes,

$$\frac{d^2\theta_\infty}{dy^2}(y) - Pr\ Rc\lambda\ \frac{d\theta_\infty}{dy}(y) + \Psi(y) = 0$$

$$\theta_\infty(0) = 0, \quad \theta_\infty(1) = 0 \tag{20}$$

The solution for the fully developed dimensionless temperature distribution, Equation 20, is given in Appendix B.

III. GENERAL METHOD OF SOLUTION

Since the fluid properties are assumed to be constant, the dimensionless momentum equation for the velocity profile, u(y), is independent of the energy equation. The solution of Equation 13 for u(y) is given in Appendix A as

$$u(y) = \frac{1}{Rc\lambda}\left[y - \frac{1 - e^{Rc\lambda y}}{1 - e^{Rc\lambda}}\right] \tag{21}$$

Hence, the dimensionless energy equation represents a linear, non-homogeneous, partial differential equation with variable coefficients subject to the given boundary conditions.

Defining a new independent variable, ξ, as the dimensionless axial coordinate scaled by the Peclet number and a new dependent variable, $\Omega(y,z)$, as the dimensionless excess temperature which is the difference between the local temperature and fully developed temperature distribution, θ_∞, as:

$$\xi = \frac{z}{P_e}$$

$$\Omega(y,\xi) = \theta(y,z) - \theta_\infty(y) \tag{22}$$

the energy equation, upon substitution of Equation 22 into Equation 14, becomes

$$u(y)\frac{\partial\Omega}{\partial\xi}(y,\xi) + P_e\lambda\frac{\partial\Omega}{dy}(y,\xi) - \frac{\partial^2\Omega}{\partial y^2}(y,\xi) - \frac{1}{Pe^2}\frac{\partial^2\Omega}{\partial\xi^2}(y,\xi)$$
$$= \left[\frac{\partial^2\theta_\infty}{\partial y^2}(y) - PrR_c\lambda\ \frac{\partial\theta_\infty}{\partial y}(y) + \Psi(y)\right] \tag{23}$$

The bracketed term on the right hand side of Equation 23 identically vanishes according to the fully developed solution of the mathematical system, Equation 20, hence the differential equation for the dimensionless excess temperature, $\Omega(y,\xi)$, reduces to a homogeneous partial differential equation with variable coefficients,

$$u(y)\frac{\partial\Omega}{\partial\xi}(y,\xi) + PrR_c\lambda\frac{\partial\Omega}{\partial y}(y,\xi) = \frac{\partial^2\Omega}{\partial y^2}(y,\xi) + \frac{1}{Pe^2}\frac{\partial^2\Omega}{\partial\xi^2}(y,\xi) \tag{24}$$

with boundary conditions:

$$\Omega(y,0) = \Omega_o(y) = \theta_o(y) - \theta_\infty(y)$$

$$\Omega(0,\xi) = 0, \quad \Omega(1,\xi) = 0$$

$$\lim_{\xi\to\infty}\ \Omega(y,\xi) = 0 \tag{25}$$

The general solution of the differential equation, Equation 24, can be constructed as an infinite series of the form:

$$\Omega(y,\xi) = \sum_{n=1}^{\infty} a^{(n)} \Omega_n(y) e^{-\beta_n \xi} \tag{26}$$

where the eigenfunctions, $\Omega_n(y)$, and the associated eigenvalues, β_n, are to be determined from the homogeneous eigenvalue problem,

$$\frac{d^2\Omega_n}{dy^2}(y) - PrR_c\lambda \frac{d\Omega_n}{dy}(y) + \left[\beta_n u(y) + \frac{\beta_n^2}{Pe^2}\right]\Omega_n(y) = 0 \tag{27}$$

with the boundary conditions

$$\Omega_n(0) = 0, \quad \Omega_n(1) = 0 \tag{28}$$

A simplification of Equation 26 is possible by defining a new set of eigenfunctions of the form,

$$F_n(y) = e^{-\frac{1}{2}PrR_c\lambda y} \Omega_n(y) \tag{29}$$

Hence the eigenvalue problem reduces to,

$$\frac{d^2F_n}{dy^2}(y) + \left[\beta_n u(y) + \frac{\beta_n^2}{Pe^2} - \frac{Pr^2R_c^2\lambda^2}{4}\right] F_n(y) = 0 \tag{30}$$

$$F_n(0) = 0, \; F_n(1) = 0$$

The general solution of the differential equation, Equation 24, becomes

$$\Omega(y,\xi) = \sum_{n=1}^{\infty} a^{(n)} F_n(y) e^{\frac{1}{2}PrR_c\lambda y} e^{-\beta_n \xi} \tag{31}$$

Since axial conduction and wall blowing effects are included, the general form of the differential equation, Equation 30, does not satisfy the conditions of the classical Sturm-Liouville system with a complete set of eigenfunctions which are orthogonal with respect to the weighing function u(y). If we assume that $F_n(y)$ and $F_m(y)$ are two characteristic functions which are solutions of Equation 30 and let β_n and β_m be the corresponding eigenvalues, assuming $m \neq n$, then the integral relation between the associated eigenfunctions becomes

$$(\beta_n - \beta_m) \int_0^1 u(y)\, F_n(y)\, F_m(y)\, dy$$

$$+ \frac{\beta_n^2 - \beta_m^2}{Pe^2} \int_0^1 F_n(y)\, F_m(y)\, dy = 0 \tag{32}$$

Equation 32 reduces to the Strum-Liouville system satisfying the property of orthogonality for the limiting case of $Pe \to \infty$, hence the present problem may be considered as a more general class of eigenvalue problem of thermal entrance regions.

CHAPTER III
APPROXIMATE SOLUTION OF THE EIGENVALUE PROBLEM BY B. G. GALERKIN METHOD

The analytical construction of the exact solutions for the eigenvalue problem of thermal entrance regions is difficult even in the case of hydrodynamic conditions with the axial conduction term and wall blowing being neglected. The eigenfunctions, for this restricted class of Sturm-Liouville systems, are obtained as infinite series of Bessel's functions of various orders which create considerable computational difficulties. Since the present problem represents a more generalized class of eigenvalue system, one expects at least the same amount of mathematical complexities in the construction of the exact solution. Although numerical solutions of the eigenfunction differential equation, Equation 30, are possible, the two point boundary conditions, together with the unknown β_n, necessitates simultaneous iterative schemes for the eigenvalues and eigenfunctions which result in extensive computational effort.

It is proposed to obtain a finite set of approximate eigenvalues and associated eigenfunctions for Equation 30 by the application of the B. G. Galerkin method. Let $\{\phi_k(y)\}$ be a selected set of functions with continuous first and second order derivatives in the range, $0 \leq y \leq 1$, that satisfy the homogeneous boundary conditions identically for all k. The selected function set must satisfy the conditions

$$\phi_k(0) = 0, \quad \phi_k(1) = 0 \quad (k = 1,2 \ldots\ldots N) \tag{33}$$

The approximate solution for $F_n(y)$ is constructed as a linear combination of the finite set of functions $\{\phi_k(y)\}$ as:

$$F_n(y) = \sum_{i=1}^{N} a_i^{(n)} \phi_i(y) = a_1^{(n)} \phi_1(y) + \ldots a_k^{(n)} \phi_N(y) \tag{34}$$

Since the set $\phi_k(y)$ identically satisfies the boundary conditions, Equation 33, for all k, $F_n(y)$ also satisfies the homogeneous boundary conditions. Substituting Equation 34 into Equation 30 gives the following,

$$\sum_{i=1}^{N} a_i^{(n)} \left\{ \frac{d^2\phi_i}{dy^2}(y) + \left[\beta_n u(y) + \frac{\beta_n^2}{Pe^2} - \frac{Pr^2 R_c^2 \lambda^2}{4} \right] \phi_i(y) \right\} = 0 \tag{35}$$

The non-dimensionalized velocity profile, u(y), is not necessarily symmetric about the channel centerline; therefore, the eigenfunctions, $F_n(y)$, are expected to yield non-symmetrical solutions. Considering the form of the boundary conditions, Equation 33, a trigonometric function set, $\{\phi_k(y)\}$, is selected as:

$$\phi_k(y) = \sin k\pi$$

$$k = 1,2,3, \ldots\ldots N \tag{36}$$

Following the method of B. G. Galerkin, that is, multiplying Equation 35 by the functions of the set, $\phi_k(y) = \sin k\pi y$, and

integrating over the range, $0 \leq y \leq 1$, the linear system of equations becomes:

$$\sum_{i=1}^{N} a_i^{(n)} \left\{ \beta_n I_1(k,i) + \left[\frac{\beta_n^2}{Pe^2} - \frac{Pr^2 R_c^2 \lambda^2}{4} - i^2\pi^2 \right] I_2(k,i) \right\} = 0 \quad (37)$$

The expressions for the integrals in Equation 37 can be obtained by analytical integration using the velocity distribution, u(y), given in Equation 21 as:

if $i \neq k$,

$$I_1(k,i) = \int_0^1 u(y) \sin i\pi y \sin k\pi y \, dy =$$

$$\frac{1}{R_c\lambda} \left\{ \frac{1 - (-1)^{i+k}}{2\pi} \left[\frac{1}{(i+k)^2} - \frac{1}{(i-k)^2} \right] - \right.$$

$$\frac{R_c\lambda}{2(e^{R_c\lambda}-1)} \left[1 - (-1)^{i+k} e^{R_c\lambda} \right] \left[\frac{1}{R_c^2\lambda^2 + (i+k)^2\pi^2} - \right.$$

$$\left. \left. \frac{1}{R_c^2\lambda^2 + (i-k)^2\pi^2} \right] \right\} \quad (38)$$

if $i = k$,

$$I_1(i,i) = \frac{1}{R_c\lambda} \left\{ \frac{1}{4} + \left(\frac{1}{2(e^{R_c\lambda}-1)} \right) \left[1 - (e^{R_c\lambda} - 1) \right. \right.$$

$$\left. \left. \left(\frac{1}{R_c\lambda} - \frac{R_c\lambda}{R_c^2\lambda^2 + 4i^2\pi^2} \right) \right] \right\} \quad (39)$$

and,

$$I_2(k,i) = \int_0^1 \sin i\pi y \sin k\pi y \, dy = \frac{1}{2}\delta_{ik} \tag{40}$$

where δ_{ik} is the Kronecker delta. Therefore, Equation 37 becomes a homogeneous system of linear equations for the undetermined linear combination constants, $a_i^{(n)}$. If a non-trivial solution is to exist for the $a_i^{(n)}$'s, hence giving $F_n(y)$ a non-trivial solution, the determinant of the coefficient matrix must vanish identically for each β_n,

$$\text{Det}\left\{\beta_n I_1(k,i) + \left[\frac{\beta_n^2}{Pe^2} - \frac{Pr^2 R_c^2 \lambda^2}{4} - i^2\pi^2\right] I_2(k,i)\right\} = 0 \tag{41}$$

Equation 41 represents a polynomial of at most 2N degree in β_n, with possibly N distinct positive roots. A set of (N-1) linearly independent equations for $a_i^{(n)}$'s exists for each β_n evaluated as a root of Equation 41 which may be solved in terms of one of the unknown linear combination constants, $a_j^{(n)}$, which will remain undetermined. Selecting the particular undetermined constant as $a_1^{(n)} = A_n$, the linear system of equations for the remaining constants $a_i^{(n)}$ becomes:

$$\sum_{i=2}^{N}\left\{\beta_n I_1(k,i) + \left[\frac{\beta_n^2}{Pe^2} - \frac{Pr^2 R_c^2 \lambda^2}{4} - i^2\pi^2\right] I_2(k,i)\right\} c_i^{(n)} =$$
$$\left\{\beta_n I_1(k,1) + \left[\frac{\beta_n^2}{Pe^2} - \frac{Pr^2 R_c^2 \lambda^2}{4} - \pi^2\right] I_2(k,1)\right\} \tag{42}$$

where

$$c_i^{(n)} = \frac{a_i^{(n)}}{a_1^{(n)}} = \frac{a_i^{(n)}}{A_n}$$

$$k = 2,3,\ldots N \tag{43}$$

Equation 42 is a non-homogeneous system of linear equations which can be solved to determine the $c_i^{(n)}$'s for each β_n evaluated as a root of Equation 41. Hence the approximate eigenfunction, $F_n(y)$, associated with β_n becomes

$$F_n(y) = A_n \sum_{i=1}^{N} c_i^{(n)} \sin i\pi y \tag{44}$$

where $c_1^{(n)} = 1$, and the $c_i^{(n)}$'s are known from the solution of Equation 42. Substituting Equation 44 into Equation 31 yields the approximate solution for the dimensionless excess temperature, $\Omega(y,\xi)$, as:

$$\Omega(y,\xi) = \sum_{n=1}^{K} A_n \left\{ e^{\frac{1}{2}PrR_c\lambda y} \sum_{i=1}^{N} c_i^{(n)} \sin i\pi y \right\} e^{-\beta_n \xi} \tag{45}$$

where K is the maximum number of distinct eigenvalues evaluated as the roots of the determinant, Equation 41.

By applying the boundary conditions given in Equation 25 the remaining K number of constants, A_n, can be determined from

$$\Omega(0,y) = \sum_{n=1}^{K} A_n \left\{ e^{\frac{1}{2}PrR_c\lambda y} \sum_{i=1}^{N} c_i^{(n)} \sin i\pi y \right\} = \Omega_o(y) \tag{46}$$

which represents the function $\Omega_o(y)$ as a linear combination of known continuous functions, $\Omega_n(y)$, in the range $0 \leq y \leq 1$. Since the finite set $\phi_i(y) = \sin i\pi y$ satisfies the necessary regularity conditions, A_n can be determined by the application of an extension of the Weierstrass approximation theorem (17). That is, multiplying Equation 46 by $\Omega_m(y)$ and integrating over $0 \leq y \leq 1$, the system of equations becomes:

$$\sum_{n=1}^{K} A_n \left[I(m,n)\right] = L(m) \tag{47}$$

where the integrals are defined as:

$$I(m,n) = \int_o^1 \left[\sum_{i=1}^{N} c_i^{(n)} \sin i\pi y \right] \left[\sum_{j=1}^{N} c_j^{(m)} \sin j\pi y \right] e^{PrR_c\lambda y} dy \tag{48}$$

$$L(m) = \int_o^1 \Omega_o(y) \left[\sum_{i=1}^{N} c_j^{(m)} \sin i\pi y \right] e^{\frac{1}{2}PrR_c\lambda y} dy \tag{49}$$

where

$$c_i^{(m)} = c_i^{(n)} = 1; \quad \Omega_o(y) = \theta_o(y) - \theta_\infty(y) \tag{50}$$

The integrals of Equations 48 and 49 may be evaluated by analytical integration using the fully developed temperature, $\theta_\infty(y)$, as presented in Appendix B.

Since $c_l^{(m)}$'s were previously determined, Equation 47 represents a non-homogeneous system of K linear equations in K unknowns which can be solved for the A_n's to complete the approximate solution for the excess temperature distribution.

CHAPTER IV
NUMERICAL RESULTS FOR THE ASSOCIATED EIGENVALUE PROBLEM

The general method, developed in the previous chapter, was applied to the associated eigenvalue problem, Equation 30, with two finite sets of trigonemetric functions, N = 8 and N = 16. Using the finite set, N = 8, the eigenvalues for all cases under consideration were obtained. A second set, N = 16, with the Peclet number, Pe = 1, was used to check the convergence of the method by comparing the results with the first set, N = 8.

The eigenvalues, β_n, were determined by evaluating the roots of the determinant containing β_n, Equation 43, by the Gaussian reduction technique on the maximum element of the matrix. Using an incremental set of β values, the determinant was evaluated within a selected β_{max} range. The approximate location of a root was indicated by a change in sign of the value of the determinant between two increments. The exact values of β_n were calculated by a controlled successive iteration scheme based on the regula-falsi method. A maximum number of twenty iterations were allowed with termination check on eight digit accuracy for two successively calculated values for each root of the eigenvalue.

The numerical calculations were performed by a CDC 1401B model computer on single precision level of eleven floating point numbers. The maximum desired values for the eigenvalues were bounded by

β_{max} = 2900 for the case of Peclet number, Pe = ∞, by β_{max} = 6000 for the case of Pe = 100, and by β_{max} = 600 for the cases of Pe = 10 and 1. These ranges of β_{max} were selected for calculation after the initial investigation of the eigenvalues with wall blowing, $R_c\lambda$ = 0.1, for the case of Pe = ∞. Except for the case, Pe = ∞, the range of β_{max} was large enough to yield 8 and 16 roots for the two finite sets of trigonemetric functions. The calculations were carried out parametrically for Prandtl number, Pr = 0.01, 0.1, 1, 10, Peclet number, Pe = ∞, 100, 10, 1, and wall blowing parameter, $R_c\lambda$ = 0.1, 1, 5, 10. For a given set of parameters Pr, Pe, and $R_c\lambda$, the average computational time required for a complete set of eigenvalues was 1.0 minutes for the function set N = 8 and 4.5 minutes for the function set N = 16.

The eigenvalues, calculated from the determinant, Equation 43, are presented in Tables I through V, for parametric values of the Peclet number, Prandtl number, and the wall blowing parameter, $R_c\lambda$.

Inspection of the data presented in Tables I through V indicates that the Peclet number has a strong effect upon the value of the eigenvalues. For the Peclet number, Pe = ∞, only three and four eigenvalues exist in the range $0 \leq \beta_n \leq 2900$, see Table I. Table II presents data for Peclet number, Pe = 100, and eight roots are noted to exist in the range $0 \leq \beta_n \leq 6000$. For the low Peclet numbers, Pe = 10 and Pe = 1, the range $0 \leq \beta_n \leq 600$ yields eight roots for the N = 8 set and sixteen roots for the N = 16 set. A comparison of a particular eigenvalue, β_1, for the various Peclet numbers shows that there is a marked decrease in the eigenvalue magnitude as the Peclet number is reduced. For the

TABLE I
EIGENVALUES FOR Pe = ∞, N = 8

		β_n			
n	Pr	$R_c\lambda = 0.1$	$R_c\lambda = 1$	$R_c\lambda = 5$	$R_c\lambda = 10$
1	0.01	9.05047(1)	9.21134(1)	1.26480(2)	2.03400(2)
2	0.01	4.31619(2)	4.39061(2)	5.95464(2)	9.31460(2)
3	0.01	1.02892(3)	1.04656(3)	1.41640(3)	2.20617(3)
4	0.01	1.88233(3)	1.91454(3)	2.58979(3)	
1	0.10	9.05050(1)	9.21365(1)	1.27262(2)	2.08364(2)
2	0.10	4.31620(2)	4.39088(2)	5.96389(2)	9.37328(2)
3	0.10	1.02892(3)	1.04659(3)	1.41739(3)	2.21245(3)
4	0.10	1.88234(3)	1.91457(3)	2.59082(3)	
1	1.0	9.05276(1)	9.44365(1)	2.04845(2)	6.81109(2)
2	1.0	4.31646(2)	4.41790(2)	6.88590(2)	1.51393(3)
3	1.0	1.02895(3)	1.04947(3)	1.51625(3)	2.83737(3)
4	1.0	1.88236(3)	1.91757(3)	2.69375(3)	
1	10.0	9.27888(1)	3.22358(2)	7.07480(3)	
2	10.0	4.34301(2)	7.09066(2)	8.43610(3)	
3	10.0	1.03170(3)	1.33630(3)	1.00050(3)	
4	10.0	1.88531(3)	2.21626(3)		

The numbers in the parentheses represent $10^{(n)}$

TABLE II
EIGENVALUES FOR Pe = 100, N = 8

		β_n			
n	Pr	$R_c\lambda = 0.1$	$R_c\lambda = 1$	$R_c\lambda = 5$	$R_c\lambda = 10$
1	0.01	8.40486(1)	8.53422(1)	1.10910(2)	1.54939(2)
2	0.01	3.20737(2)	3.23936(2)	3.79159(2)	4.49716(2)
3	0.01	6.05883(2)	6.10039(2)	6.78216(2)	7.58133(2)
4	0.01	9.04658(2)	9.09314(2)	9.84295(2)	1.06941(3)
5	0.01	1.20875(3)	1.21374(3)	1.29333(3)	1.38189(3)
6	0.01	1.51554(3)	1.52089(3)	1.60436(3)	1.69500(3)
7	0.01	1.83986(3)	1.84438(3)	1.92000(3)	2.00883(3)
8	0.01	2.15079(3)	2.15650(3)	2.24295(3)	2.33185(3)
1	0.10	8.40488(1)	8.53621(1)	1.11522(2)	1.58011(2)
2	0.10	3.20738(2)	3.23952(2)	3.79595(2)	4.51588(2)
3	0.10	6.05883(2)	6.10051(2)	6.78529(2)	7.59420(2)
4	0.10	9.04658(2)	9.09324(2)	9.84535(2)	1.07038(3)
5	0.10	1.20875(3)	1.21375(3)	1.29352(3)	1.38267(3)
6	0.10	1.51554(3)	1.52089(3)	1.60452(3)	1.69566(3)
7	0.10	1.83986(3)	1.84439(3)	1.92014(3)	2.00939(3)
8	0.10	2.15079(3)	2.15651(3)	2.24308(3)	2.33235(3)
1	1.0	8.40684(1)	8.73451(1)	1.69123(2)	3.92222(2)
2	1.0	3.20753(2)	3.25542(2)	4.21879(2)	6.17795(2)
3	1.0	6.05895(2)	6.11247(2)	7.09277(2)	8.84479(2)
4	1.0	9.04667(2)	9.10261(2)	1.00829(3)	1.16431(3)
5	1.0	1.20876(3)	1.21451(3)	1.31279(3)	1.45908(3)
6	1.0	1.51555(3)	1.52154(3)	1.62070(3)	1.75993(3)
7	1.0	1.83987(3)	1.84995(3)	1.93409(3)	2.06479(3)
8	1.0	2.15079(3)	2.15700(3)	2.25539(3)	2.38124(3)
1	10.0	8.60264(1)	2.60327(2)	2.12674(3)	4.72485(3)
2	10.0	3.22333(2)	4.70391(2)	2.25070(3)	4.81060(3)
3	10.0	6.07087(2)	7.24537(2)	2.37492(3)	4.88838(3)
4	10.0	9.05603(2)	1.00082(3)	2.50961(3)	4.96462(3)
5	10.0	1.20952(3)	1.28920(3)	2.66530(3)	5.05057(3)
6	10.0	1.51619(3)	1.58482(3)	2.84497(3)	5.15268(3)
7	10.0	1.84043(3)	1.90026(3)	3.04767(3)	5.27047(3)
8	10.0	2.15128(3)	2.20570(3)	3.27985(3)	5.42832(3)

The numbers in the parentheses represent $10^{(n)}$

TABLE III
EIGENVALUES FOR Pe = 10, N = 8

		β_n			
n	Pr	$R_c\lambda$ = 0.1	$R_c\lambda$ = 1	$R_c\lambda$ = 5	$R_c\lambda$ = 10
1	0.01	2.64449(1)	2.65257(1)	2.77959(1)	2.91402(1)
2	0.01	5.84972(1)	5.85633(1)	5.95883(1)	6.06866(1)
3	0.01	9.00428(1)	9.01076(1)	9.11090(1)	9.21679(1)
4	0.01	1.21497(2)	1.21562(2)	1.22564(2)	1.23616(2)
5	0.01	1.52927(2)	1.52992(2)	1.53998(2)	1.55050(2)
6	0.01	1.84348(2)	1.84414(2)	1.85424(2)	1.86476(2)
7	0.01	2.15787(2)	2.15852(2)	2.16852(2)	2.17900(2)
8	0.01	2.47204(2)	2.47270(2)	2.48281(2)	2.49330(2)
1	0.10	2.64449(1)	2.65296(1)	2.78935(1)	2.95304(1)
2	0.10	5.84972(1)	5.85652(1)	5.96375(1)	6.08832(1)
3	0.10	9.00428(1)	9.01089(1)	9.11418(1)	9.22991(1)
4	0.10	1.21497(2)	1.21563(2)	1.22589(2)	1.23715(2)
5	0.10	1.52927(2)	1.52993(2)	1.54018(2)	1.55129(2)
6	0.10	1.84348(2)	1.84414(2)	1.85440(2)	1.86542(2)
7	0.10	2.15787(2)	2.15852(2)	2.16866(2)	2.17956(2)
8	0.10	2.47204(2)	2.47270(2)	2.48294(2)	2.49397(2)
1	1.0	2.64488(1)	2.69155(1)	3.64735(1)	5.67200(1)
2	1.0	5.84991(1)	5.87614(1)	6.43731(1)	7.81454(1)
3	1.0	9.00442(1)	9.02399(1)	9.43664(1)	1.04606(2)
4	1.0	1.21498(2)	1.21661(2)	1.25026(2)	1.33196(2)
5	1.0	1.52928(2)	1.53072(2)	1.55975(2)	1.62815(2)
6	1.0	1.84349(2)	1.84480(2)	1.87074(2)	1.92994(2)
7	1.0	2.15788(2)	2.15909(2)	2.18268(2)	2.23512(2)
8	1.0	2.47205(2)	2.47320(2)	2.49522(2)	2.54255(2)
1	10.0	2.68345(1)	5.39442(1)	2.48045(2)	4.98478(2)
2	10.0	5.86952(1)	7.59931(1)	2.54481(2)	5.01800(2)
3	10.0	9.01752(1)	1.02538(2)	2.64012(2)	5.06728(2)
4	10.0	1.21596(2)	1.31139(2)	2.76692(2)	5.13500(2)
5	10.0	1.53006(2)	1.60756(2)	2.92161(2)	5.22061(2)
6	10.0	1.84414(2)	1.90931(2)	3.10020(2)	5.32329(2)
7	10.0	2.15844(2)	2.21464(2)	3.29898(2)	5.44213(2)
8	10.0	2.47254(2)	2.52014(2)	3.51451(2)	5.57627(2)

The numbers in the parentheses represent $10^{(n)}$

TABLE IV
EIGENVALUES FOR Pe = 1, N = 8

		β_n			
n	Pr	$R_c\lambda = 0.1$	$R_c\lambda = 1$	$R_c\lambda = 5$	$R_c\lambda = 10$
1	0.01	3.08773(0)	3.08870(0)	3.10347(0)	3.11848(0)
2	0.01	6.23850(0)	6.23919(0)	6.24992(0)	6.26149(0)
3	0.01	9.38181(0)	9.38248(0)	9.39287(0)	9.40383(0)
4	0.01	1.25239(1)	1.25246(1)	1.25350(1)	1.25458(1)
5	0.01	1.56658(1)	1.56665(1)	1.56768(1)	1.56875(1)
6	0.01	1.88075(1)	1.88082(1)	1.88185(1)	1.88293(1)
7	0.01	2.19492(1)	2.19499(1)	2.19026(1)	2.19709(1)
8	0.01	2.50909(1)	2.50916(1)	2.51019(1)	2.51126(1)
1	0.10	3.08773(0)	3.08909(0)	3.11331(0)	3.15762(0)
2	0.10	6.23850(0)	6.23939(0)	6.25484(0)	6.28115(0)
3	0.10	9.38181(0)	9.38261(0)	9.39616(0)	9.41696(0)
4	0.10	1.25239(1)	1.25247(1)	1.25374(1)	1.25556(1)
5	0.10	1.56658(1)	1.56666(1)	1.56788(1)	1.56954(1)
6	0.10	1.88075(1)	1.88083(1)	1.88202(1)	1.88358(1)
7	0.10	2.19492(1)	2.19500(1)	2.19616(1)	2.19765(1)
8	0.10	2.50909(1)	2.50916(1)	2.51031(1)	2.51175(1)
1	1.0	3.08813(0)	3.12823(0)	3.97665(0)	5.88148(0)
2	1.0	6.25905(0)	6.25905(0)	6.72896(0)	8.00794(0)
3	1.0	9.38194(0)	9.39573(0)	9.71878(0)	1.06478(1)
4	1.0	1.25240(1)	1.25346(1)	1.27812(1)	1.35038(1)
5	1.0	1.56659(1)	1.56744(1)	1.58745(1)	1.64640(1)
6	1.0	1.88076(1)	1.88148(1)	1.89836(1)	1.94811(1)
7	1.0	2.19493(1)	2.19556(1)	2.21018(1)	2.25321(1)
8	1.0	2.50909(1)	2.50965(1)	2.52259(1)	2.56051(1)
1	10.0	3.12726(0)	5.85193(0)	2.51580(1)	5.00748(1)
2	10.0	6.25836(0)	7.98581(0)	2.57441(1)	5.03713(1)
3	10.0	9.39506(0)	1.06266(1)	2.66855(1)	5.08594(1)
4	10.0	1.25339(1)	1.34828(1)	2.79491(1)	5.15342(1)
5	10.0	1.56738(1)	1.64431(1)	2.94940(1)	5.23889(1)
6	10.0	1.88142(1)	1.94601(1)	3.12788(1)	5.34147(1)
7	10.0	2.19549(1)	2.25511(1)	3.32649(1)	5.46022(1)
8	10.0	2.50959(1)	2.55841(1)	3.54185(1)	5.59410(1)

The numbers in the parentheses represent $10^{(n)}$

TABLE V
EIGENVALUES FOR Pe = 1, N = 16

		β_n			
n	Pr	$R_C\lambda = 0.1$	$R_C\lambda = 1$	$R_C\lambda = 5$	$R_C\lambda = 10$
1	0.01	3.08773(0)	3.08870(0)	3.10347(0)	3.11848(0)
2	0.01	6.23850(0)	6.23919(0)	6.24992(0)	6.26149(0)
3	0.01	9.38181(0)	9.38248(0)	9.39287(0)	9.40383(0)
4	0.01	1.25239(1)	1.25246(1)	1.25350(1)	1.25458(1)
5	0.01	1.56665(1)	1.56665(1)	1.56768(1)	1.56875(1)
6	0.01	1.88075(1)	1.88082(1)	1.88185(1)	1.88293(1)
7	0.01	2.19492(1)	2.19499(1)	2.19602(1)	2.19709(1)
8	0.01	2.50909(1)	2.50915(1)	2.51019(1)	2.51126(1)
9	0.01	2.82325(1)	2.82332(1)	2.82435(1)	2.82542(1)
10	0.01	3.13741(1)	3.13748(1)	3.13851(1)	3.13958(1)
11	0.01	3.45157(1)	3.45164(1)	3.45267(1)	3.45374(1)
12	0.01	3.76573(1)	3.76580(1)	3.76683(1)	3.76790(1)
13	0.01	4.07989(1)	4.07996(1)	4.08206(1)	4.08206(1)
14	0.01	4.39405(1)	4.39412(1)	4.39515(1)	4.39622(1)
15	0.01	4.70822(1)	4.70828(1)	4.70931(1)	4.71038(1)
16	0.01	5.02238(1)	5.02244(1)	5.02347(1)	5.02454(1)
1	0.10	3.08773(0)	3.08909(0)	3.11331(0)	3.15762(0)
2	0.10	6.23850(0)	6.23939(0)	6.25484(0)	6.28115(0)
3	0.10	9.38181(0)	9.38261(0)	9.39616(0)	9.31696(0)
4	0.10	1.25239(1)	1.25247(1)	1.25374(1)	1.25556(1)
5	0.10	1.56658(1)	1.56666(1)	1.56788(1)	1.56954(1)
6	0.10	1.88075(1)	1.88083(1)	1.88202(1)	1.88358(1)
7	0.10	2.19492(1)	2.19500(1)	2.19616(1)	2.19765(1)
8	0.10	2.50909(1)	2.50916(1)	2.51031(1)	2.51175(1)
9	0.10	2.82325(1)	2.82332(1)	2.82446(1)	2.82586(1)
10	0.10	3.13741(1)	3.13748(1)	3.13861(1)	3.13997(1)
11	0.10	3.45157(1)	3.45164(1)	3.45276(1)	3.45410(1)
12	0.10	3.76573(1)	3.76580(1)	3.76691(1)	3.76823(1)
13	0.10	4.07989(1)	4.07996(1)	4.08107(1)	4.08236(1)
14	0.10	4.39405(1)	4.39412(1)	4.39522(1)	4.39650(1)
15	0.10	4.70822(1)	4.70829(1)	4.70938(1)	4.71064(1)
16	0.10	5.02238(1)	5.02245(1)	5.02353(1)	5.02479(1)

TABLE V (Continued)

		β_n			
n	Pr	$R_c\lambda = 0.1$	$R_c\lambda = 1$	$R_c\lambda = 5$	$R_c\lambda = 10$
1	1.0	3.08813(0)	3.12823(0)	3.97665(0)	5.88148(0)
2	1.0	6.23870(0)	6.25905(0)	6.72896(0)	8.00794(0)
3	1.0	9.38194(0)	9.39573(0)	9.71878(0)	1.06478(1)
4	1.0	1.25240(1)	1.25346(1)	1.27812(1)	1.35038(1)
5	1.0	1.56659(1)	1.56744(1)	1.58745(1)	1.64640(1)
6	1.0	1.88076(1)	1.88148(1)	1.89836(1)	1.94811(1)
7	1.0	2.19493(1)	2.19556(1)	2.21018(1)	2.25321(1)
8	1.0	2.50909(1)	2.50965(1)	2.52259(1)	2.56050(1)
9	1.0	2.82325(1)	2.82376(1)	2.83538(1)	2.86928(1)
10	1.0	3.13742(1)	3.13788(1)	3.14844(1)	3.17912(1)
11	1.0	3.45158(1)	3.45200(1)	3.46170(1)	3.48972(1)
12	1.0	3.76574(1)	3.76613(1)	3.77511(1)	3.80091(1)
13	1.0	4.07990(1)	4.08027(1)	4.08864(1)	4.11255(1)
14	1.0	4.39406(1)	4.39441(1)	4.40225(1)	4.42455(1)
15	1.0	4.70822(1)	4.70855(1)	4.71594(1)	4.73683(1)
16	1.0	5.02238(1)	5.02269(1)	5.02969(1)	5.04935(1)
1	10.0	3.12726(0)	5.85193(0)	2.51580(1)	5.00748(1)
2	10.0	6.25836(0)	7.98581(0)	2.57441(1)	5.03713(1)
3	10.0	9.39506(0)	1.06266(1)	2.66855(1)	5.08594(1)
4	10.0	1.25339(1)	1.34828(1)	2.79491(1)	5.15342(1)
5	10.0	1.56738(1)	1.64431(1)	2.94940(1)	5.23889(1)
6	10.0	1.88142(1)	1.94601(1)	3.12788(1)	5.34147(1)
7	10.0	2.19549(1)	2.25111(1)	3.32648(1)	5.46021(1)
8	10.0	2.50958(1)	2.55841(1)	3.54184(1)	5.59410(1)
9	10.0	2.82369(1)	2.86719(1)	3.77109(1)	5.74205(1)
10	10.0	3.13781(1)	3.17702(1)	4.01184(1)	5.90303(1)
11	10.0	3.45194(1)	3.48762(1)	4.26215(1)	6.07600(1)
12	10.0	3.76607(1)	3.79881(1)	4.52044(1)	6.25995(1)
13	10.0	4.08020(1)	4.11045(1)	4.78541(1)	6.45396(1)
14	10.0	4.39434(1)	4.42245(1)	5.05602(1)	6.65715(1)
15	10.0	4.70848(1)	4.73474(1)	5.33140(1)	6.86870(1)
16	10.0	5.02262(1)	5.04725(1)	5.61084(1)	7.08786(1)

The numbers in the parentheses represent $10^{(n)}$

low Peclet number, Pe = 1, the N = 16 set provides twice the number of eigenvalues as the N = 8 set in the range $0 \leq \beta_n \leq 600$ with the approximate maximum value, $\beta_{max} = 50$. Since the magnitude of the eigenvalues is the controlling factor in determining the truncation point in the infinite series solution, Equation 26, the calculations for the temperature development may be in considerable error, if the number of eigenvalues is not sufficient to assure the convergence.

The wall blowing parameter, $R_c\lambda$, is noted to also have considerable effect on the magnitude of the eigenvalues for a particular combination of Peclet and Prandtl numbers. The magnitude of β tends to increase as the value of the wall blowing parameter increases. Inspection of the data presented in Tables I and II for Peclet numbers, Pe = ∞ and 100, reveals that there is a relatively large increase in the values of the eigenvalues as the wall blowing parameter increases from $R_c\lambda$ = 0.1 to $R_c\lambda$ = 10. In Table I for Prandtl number, Pr = 1, the eigenvalue, β_1, is seen to increase from approximately 90 to 680 as the wall blowing parameter increases from 0.1 to 10. It is also noted that the change in magnitude of the eigenvalue with respect to the wall blowing parameter is increased as the Prandtl number changes from Pr = 0.01 to Pr = 10. These same effects are noticed but to a lesser extent in Tables III through V, for Peclet numbers, Pe = 10 and 1. In Table IV for Prandtl number, Pr = 1, the eigenvalue, β_1, is seen to increase from approximately 3 to 6 as the wall blowing parameter increases from 0.1 to 10. For the large values of wall blowing parameter and Prandtl number, $R_c\lambda$ = 10 and Pr = 10, Tables III and IV indicate a small difference in value for

successive eigenvalues within the finite set of functions, N = 8. The range for Peclet numbers, Pe = 10 and 1, is, respectively, $49.8 < \beta_n < 55.8$ and $50.0 < \beta_n < 55.9$ for the first eight eigenvalues.

One of the interesting characteristics of the present method is that the eight eigenvalues, which is the maximum number that can be evaluated from an eight by eight determinant, compare extremely well with the first eight eigenvalues evaluated from the N = 16 set, for the case of Pe = 1. Hence, it is sufficient to start the solution for the eigenvalue problem with the N = 8 set, and later increase the number of approximating set to N = 16 if it becomes necessary to calculate additional eigenvalues.

CHAPTER V
ENTRANCE REGION TEMPERATURE DEVELOPMENT

The eigenvalues evaluated by the B. G. Galerkin method in the previous chapter were used to determine the temperature development under constant wall temperature conditions for a specified uniform entrance temperature, $T_o(x_2) = T_o^*$. The linear combination constants, $c_i^{(n)}$, associated with the eigenfunction, $F_n(y)$, were evaluated from the reduced system of linear equations, Equation 42. For each particular value of β_n a set of $c_i^{(n)}$'s was obtained by use of the Gaussian reduction technique on the pivotal element of the coefficient matrix.

The analytic and approximate solutions for the fully developed temperature, $\theta_\infty(y)$, are given in Appendix B. The approximate B. G. Galerkin method solution,

$$\theta_\infty(y) = PrEc\, e^{\frac{1}{2}PrR_c\lambda y} \sum_{i=1}^{M} D_i \sin i\pi y \tag{51}$$

was used since an extensive simplification in the evaluation of the required integrals for the A_n's was possible. In the present study, twenty terms were used to determine the fully developed temperature given in Equation 51. The final form of the dimensionless excess temperature, Equation 45, becomes,

$$\Omega(y,\xi) = \theta(y,\xi) - \theta_\infty(y) = \frac{T(y,\xi) - T_w}{T_o^* - T_w} - \frac{T_\infty(y) - T_w}{T_o^* - T_w} \tag{52}$$

or,

$$\frac{T(y,\xi) - T_w}{T_o^* - T_w} = \sum_{n=1}^{K} A_n \left\{ e^{\frac{1}{2}PrR_c\lambda y} \sum_{i=1}^{N} c_i^{(n)} \sin i\pi y \right\} e^{-\beta_n \xi}$$

$$+ PrEc\, e^{\frac{1}{2}PrR_c\lambda y} \sum_{i=1}^{M} D_i \sin i\pi y \qquad (53)$$

The system of simultaneous equations for the evaluation of the A_n's is from Equation 47

$$\sum_{n=1}^{K} A_n [I(m,n)] = L(m)$$

Following the general procedure as outlined in Chapter III, the necessary integrals for the evaluation of the A_n's by the Weierstrass approximation theorem are evaluated by analytical integration as,

$$I(m,n) = \int_0^1 \left[\sum_{i=1}^{N} c_i^{(n)} \sin i\pi y \right] \left[\sum_{j=1}^{N} c_j^{(m)} \sin j\pi y \right] e^{PrR_c\lambda y}\, dy =$$

$$\sum_{i=1}^{N} \sum_{j=1}^{N} c_i^{(n)}\, c_j^{(m)} \left\{ \frac{PrR_c\lambda}{2} \left[(-1)^{i+j}\, e^{PrR_c\lambda} - 1 \right] \cdot \right.$$

$$\left. \left[\frac{1}{(PrR_c\lambda)^2 + (i-j)^2\pi^2} - \frac{1}{(PrR_c\lambda)^2 + (i+j)^2\pi^2} \right] \right\} \qquad (54)$$

and

$$L(m) = \int_0^1 \left[1 - PrEc e^{\frac{1}{2}PrR_c\lambda y} \sum_{i=1}^{M} D_i \sin i\pi y\right]\left[\sum_{j=1}^{N} c_j^{(m)} \sin j\pi y\right] e^{\frac{1}{2}PrR_c\lambda y}\, dy =$$

$$\sum_{j=1}^{N} c_j^{(m)} \left\{\frac{-4j\pi}{(PrR_c\lambda)^2 + 4j^2\pi^2}\left[(-1)^j e^{\frac{1}{2}PrR_c\lambda} - 1\right]\right\} -$$

$$PrEc \sum_{i=1}^{M} \sum_{j=1}^{N} c_j^{(m)} D_i \left\{\frac{PrR_c\lambda}{2}\left[(-1)^{i+j} e^{PrR_c\lambda} - 1\right] \cdot \right.$$

$$\left. \left[\frac{1}{(PrR_c\lambda)^2 + (i-j)^2\pi^2} - \frac{1}{(PrR_c\lambda)^2 + (i+j)^2\pi^2}\right]\right\} \qquad (55)$$

where,

$$c_i^{(m)} = c_i^{(n)} = 1 \qquad (56)$$

from the definition of the eigenfunctions $\Omega_n(y)$, and constants, A_n. Since the linear combination constants, $c_i^{(n)}$, are completely determined for the set of eigenfunctions, the integrals, Equation 54 and Equation 55, are readily evaluated for solution of A_n's from the system of linear equations.

The system of linear equations was solved by the Gaussian reduction scheme for various values of the parameters Pr, PrEc, and $R_c\lambda$. The excess temperature was evaluated at twenty-one points across the channel for different axial locations, ξ.

The development of the dimensionless temperature, $\theta(y,\xi)$, along the channel is presented in Figures 2 through 12 for various values of wall blowing parameter, $R_c\lambda$, Prandtl number, Pr, and the product of the Prandtl and the pseudo Eckert numbers, PrEc. For various axial locations, ξ, profiles are given for values of the Peclet number, Pe = ∞, 100, 10, and 1.

The effect of the wall blowing parameter on the dimensionless temperature profiles is shown in Figures 2 through 10 for Prandtl number, Pr = 1. The hydrodynamic case with no wall blowing is approximated by the conditions presented in Figures 2 through 4. It is noted that these conditions, in which $R_c\lambda = 0.1$, produce profiles which are approximately symmetrical about the channel centerline. Inspection of the data presented in Figures 5 through 9 shows that the excess temperature profiles become more non-symmetrical as the wall blowing parameter increases from $R_c\lambda = 1$ to $R_c\lambda = 10$. The maximum value of excess temperature for all axial coordinate positions, ξ, is observed to be displaced toward the upper channel wall at y = 1. This result is to be expected due to the injection of fluid through the lower channel wall, y = 0, with a temperature of T_w. From Figure A-1, page 73, the wall blowing parameter is noted to displace the velocity profile toward the upper channel wall, producing greater velocity gradients near this wall. The displacement of the velocity profiles results in greater heating due to viscous effects in the region near the upper wall of the channel, which also tends to produce non-symmetrical temperature profiles. Inspection of the data indicates that the wall blowing parameter tends to decrease the magnitude

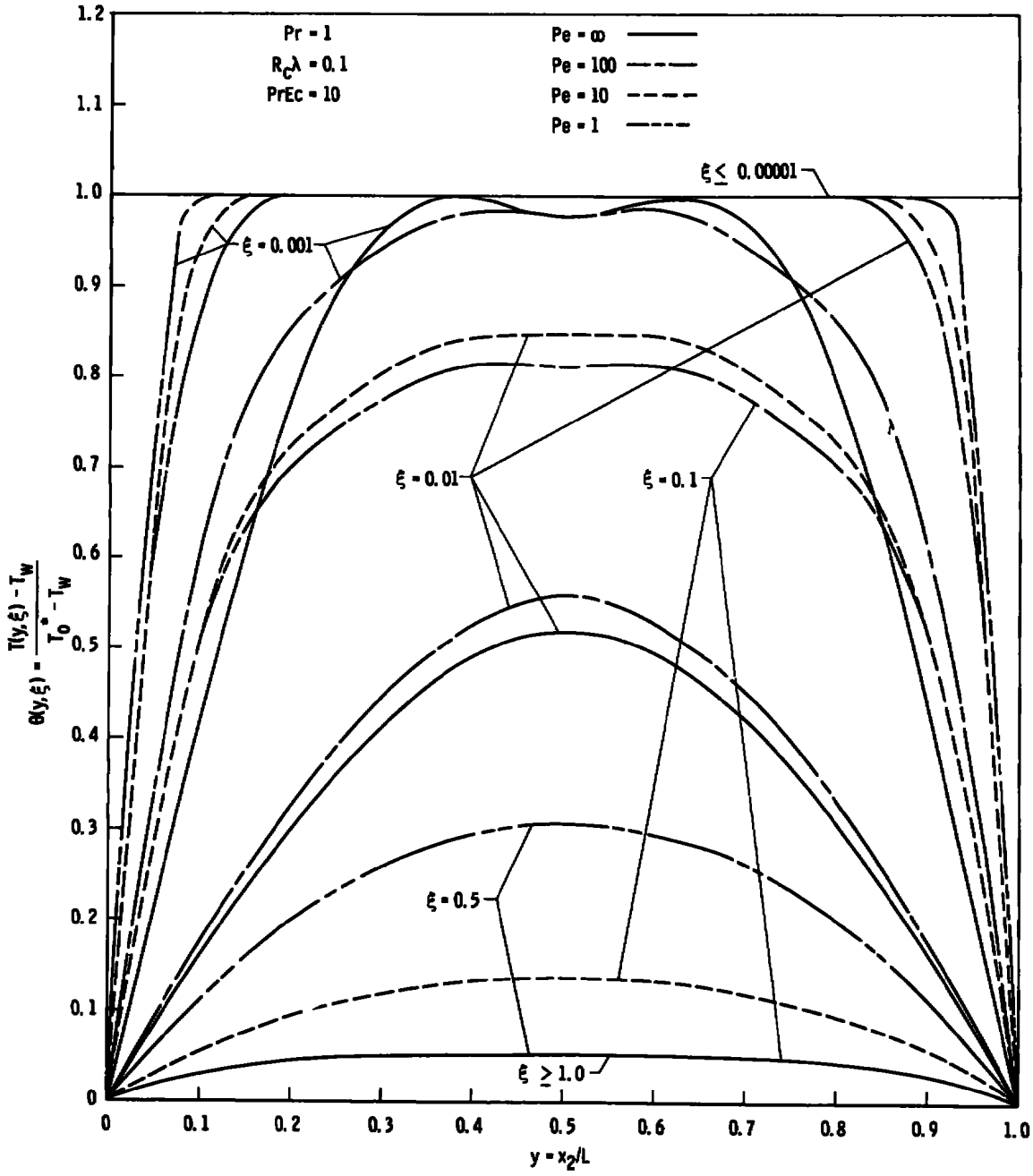

Fig. 2 Temperature Profiles; Pr = 1, $R_c\lambda$ = 0.1, PrEc = 10

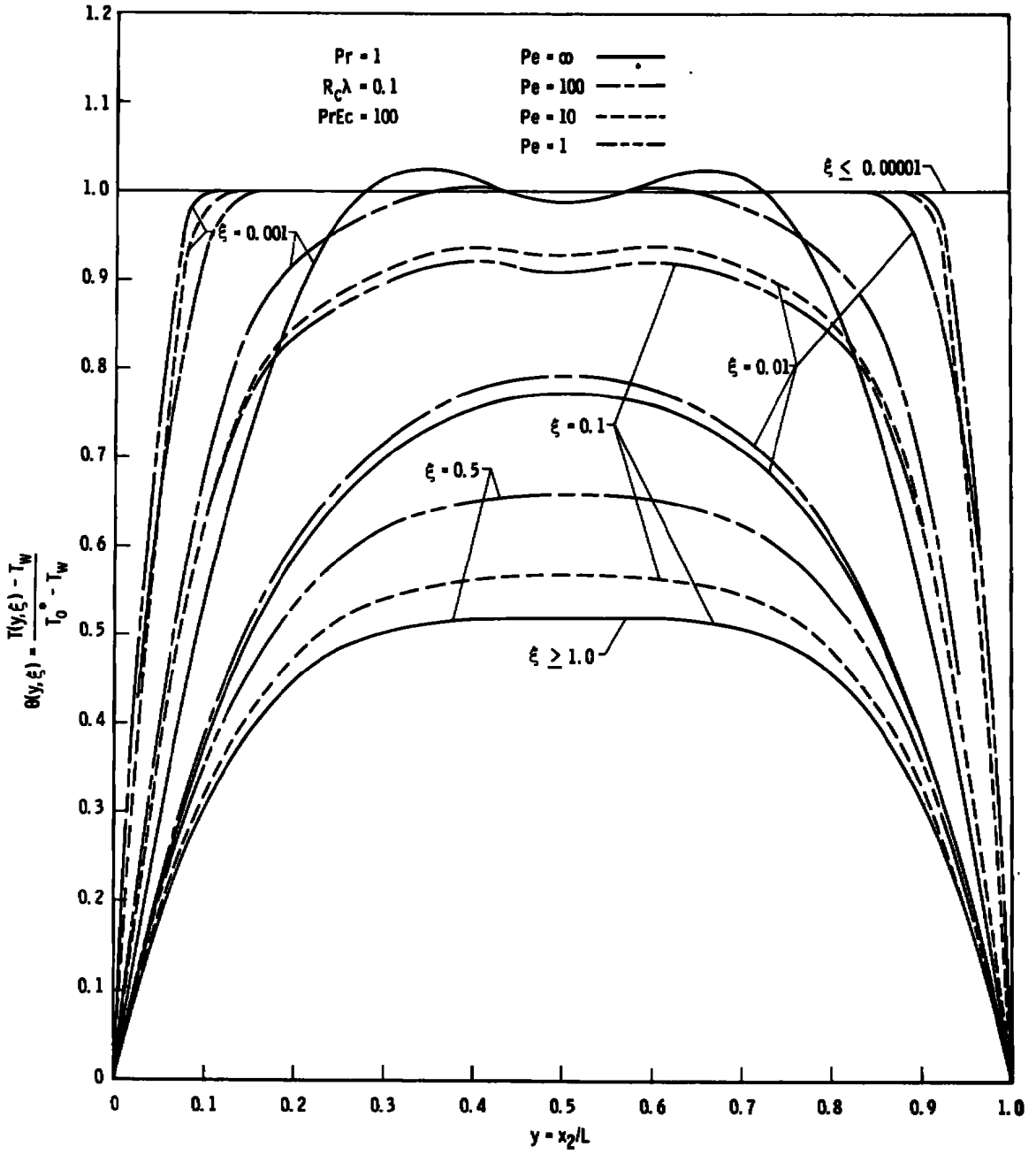

Fig. 3 Temperature Profiles; Pr = 1, $R_c\lambda$ = 0.1, PrEc = 100

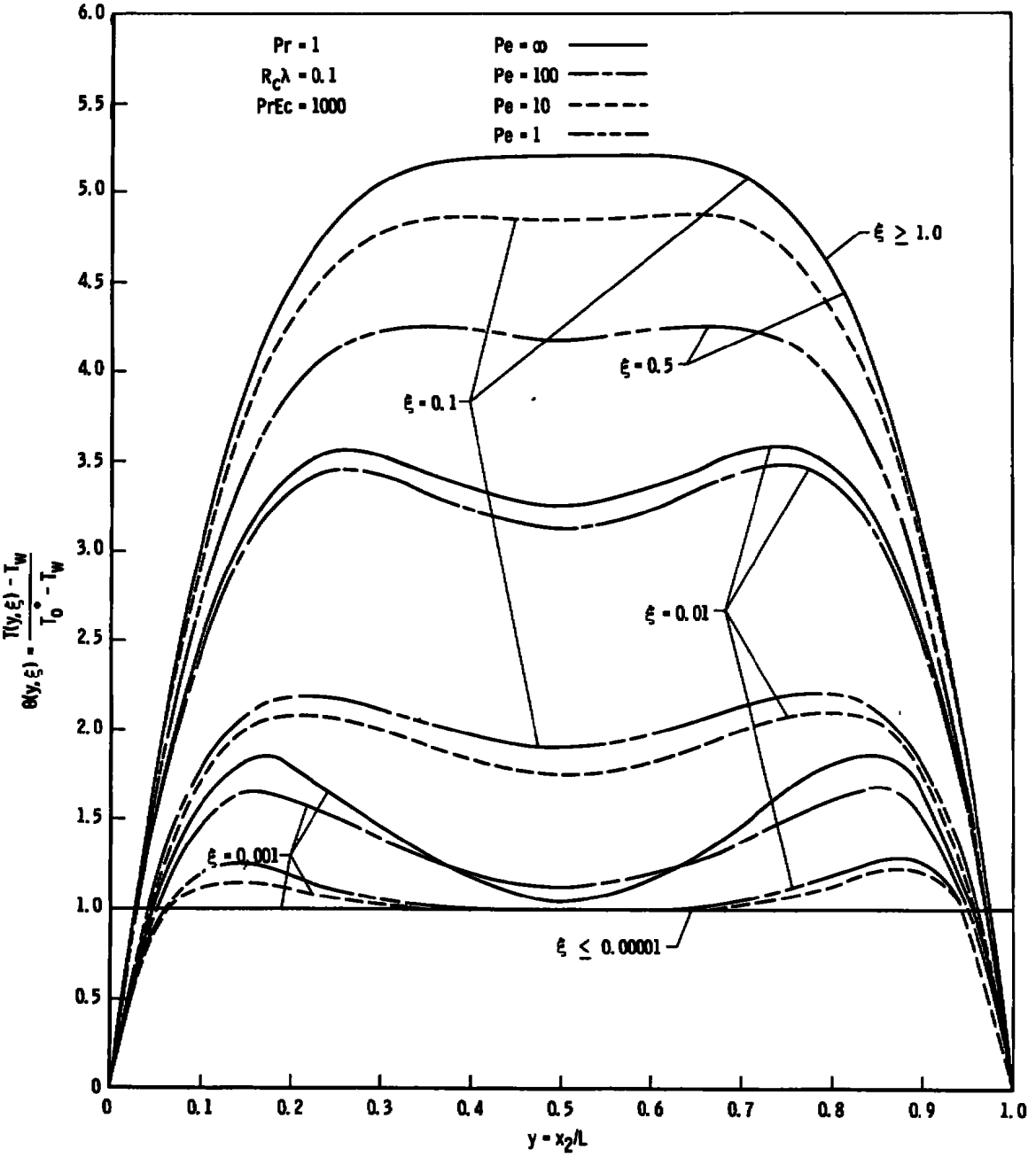

Fig. 4 Temperature Profiles; Pr = 1, $R_c\lambda$ = 0.1, PrEc = 1000

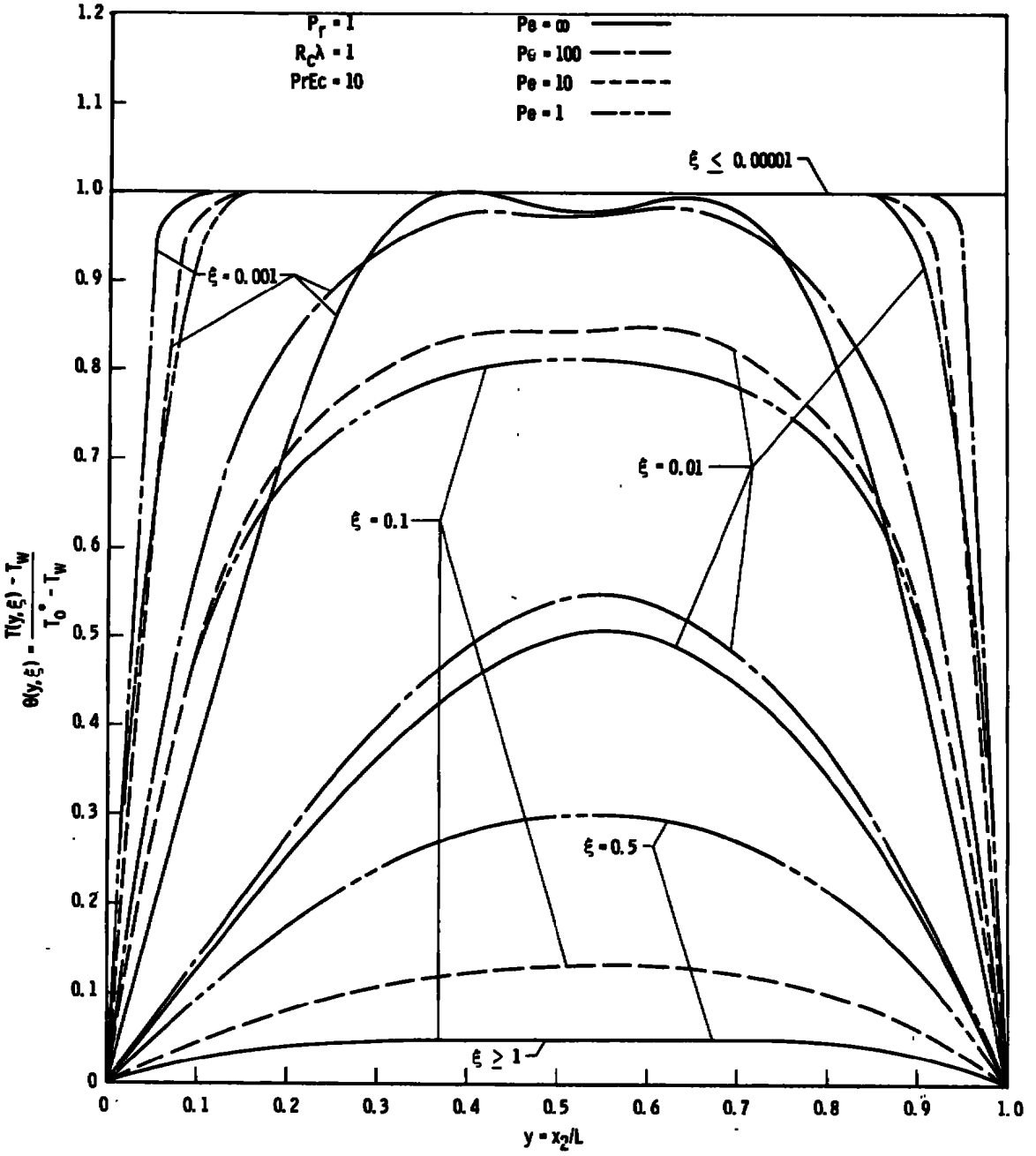

Fig. 5 Temperature Profiles; Pr = 1, $R_e\lambda$ = 1, PrEc = 10

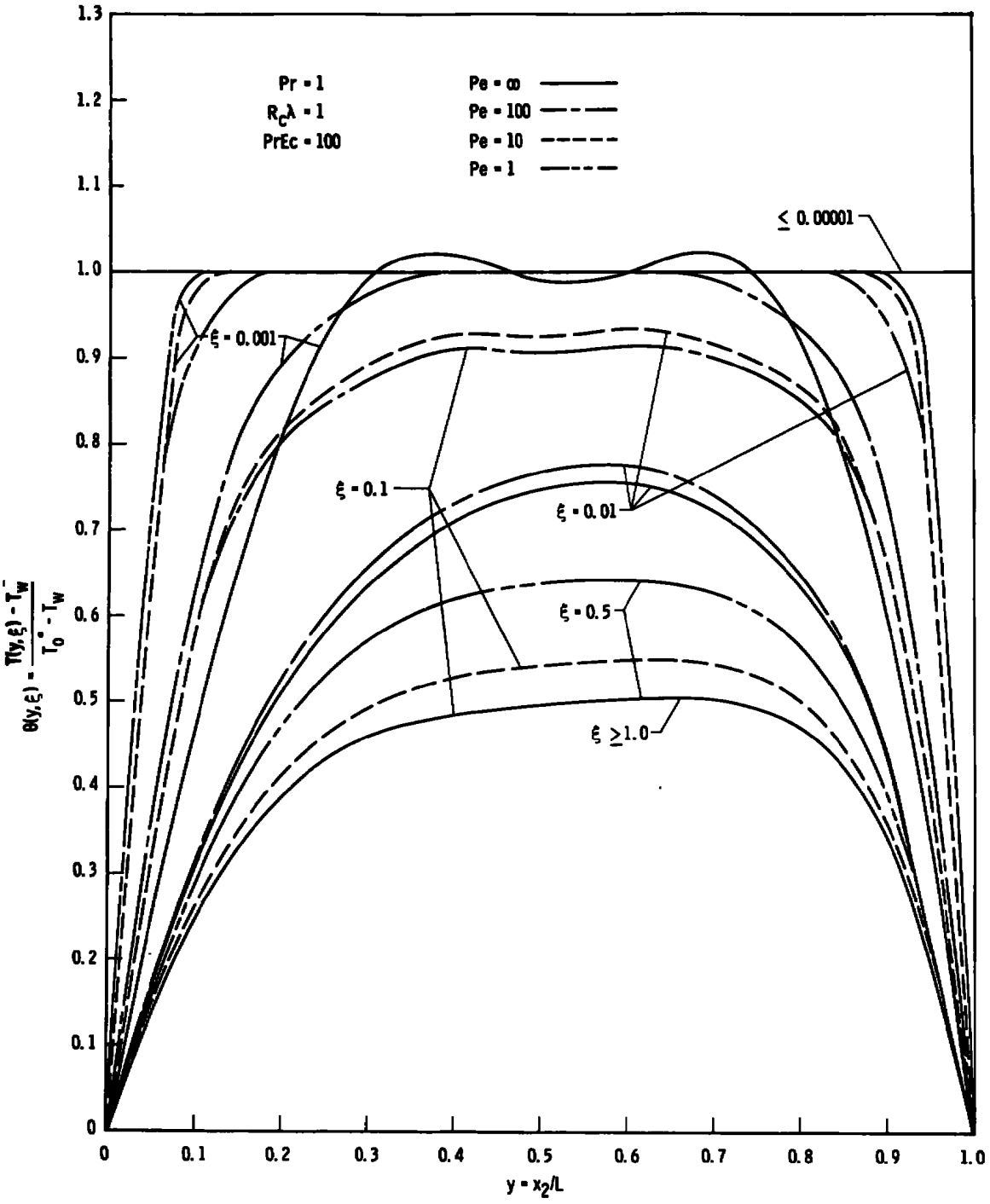

Fig. 6 Temperature Profiles; Pr = 1, $R_c\lambda$ = 1, PrEc = 100

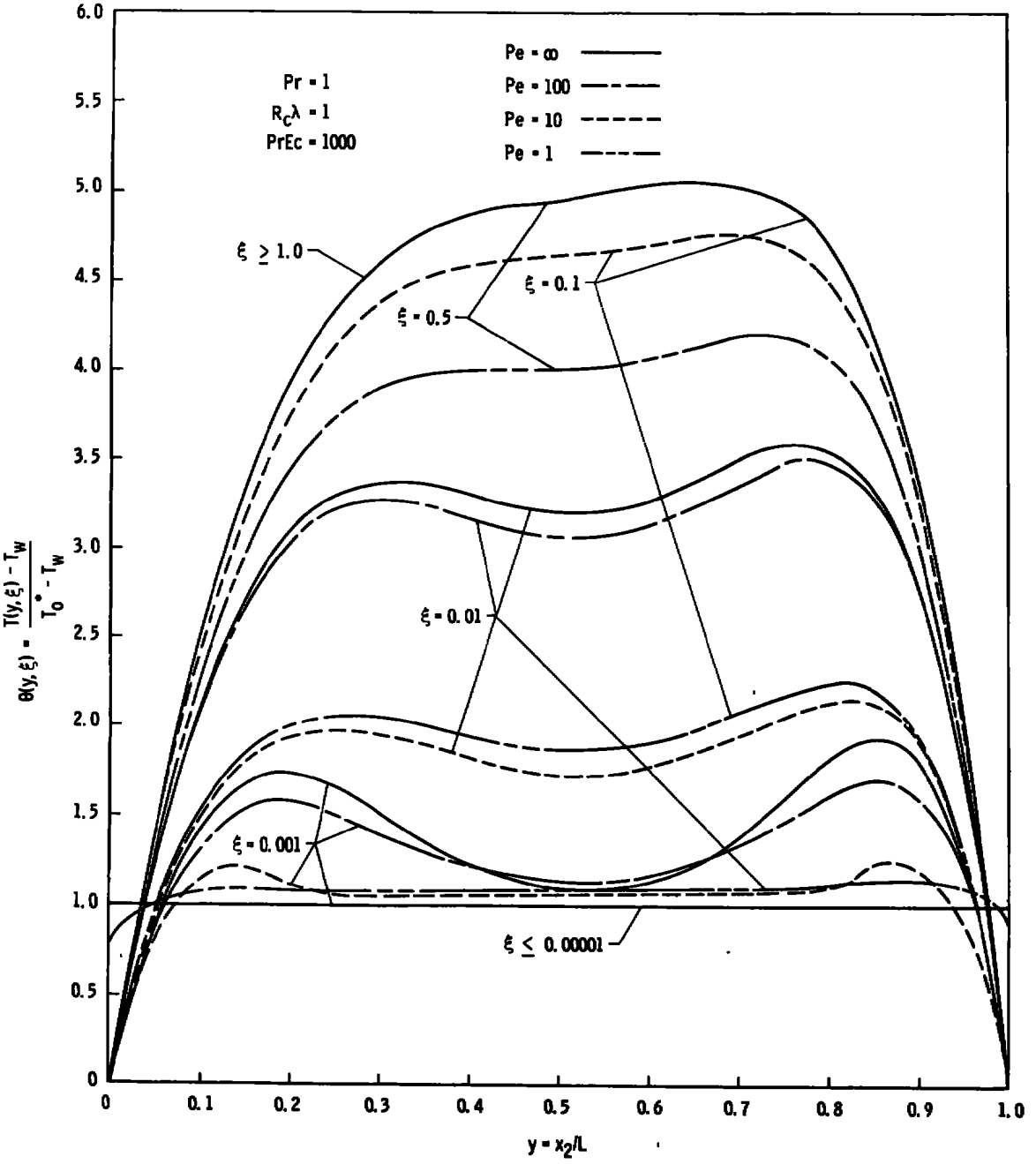

Fig. 7 Temperature Profiles; Pr = 1, $R_c\lambda$ = 1, PrEc = 1000

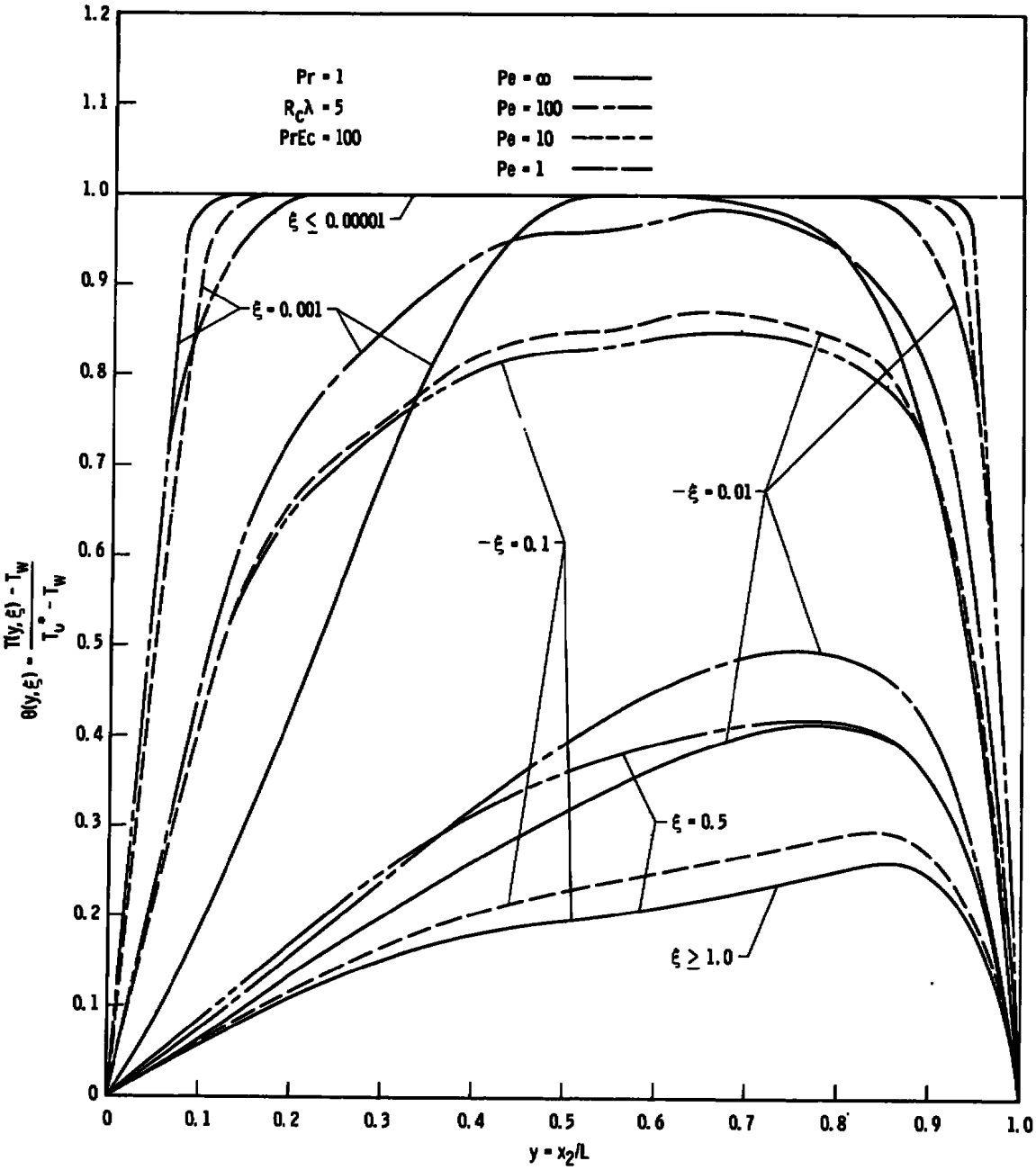

Fig. 8 Temperature Profiles; Pr = 1, $R_c\lambda$ = 5, PrEc = 100

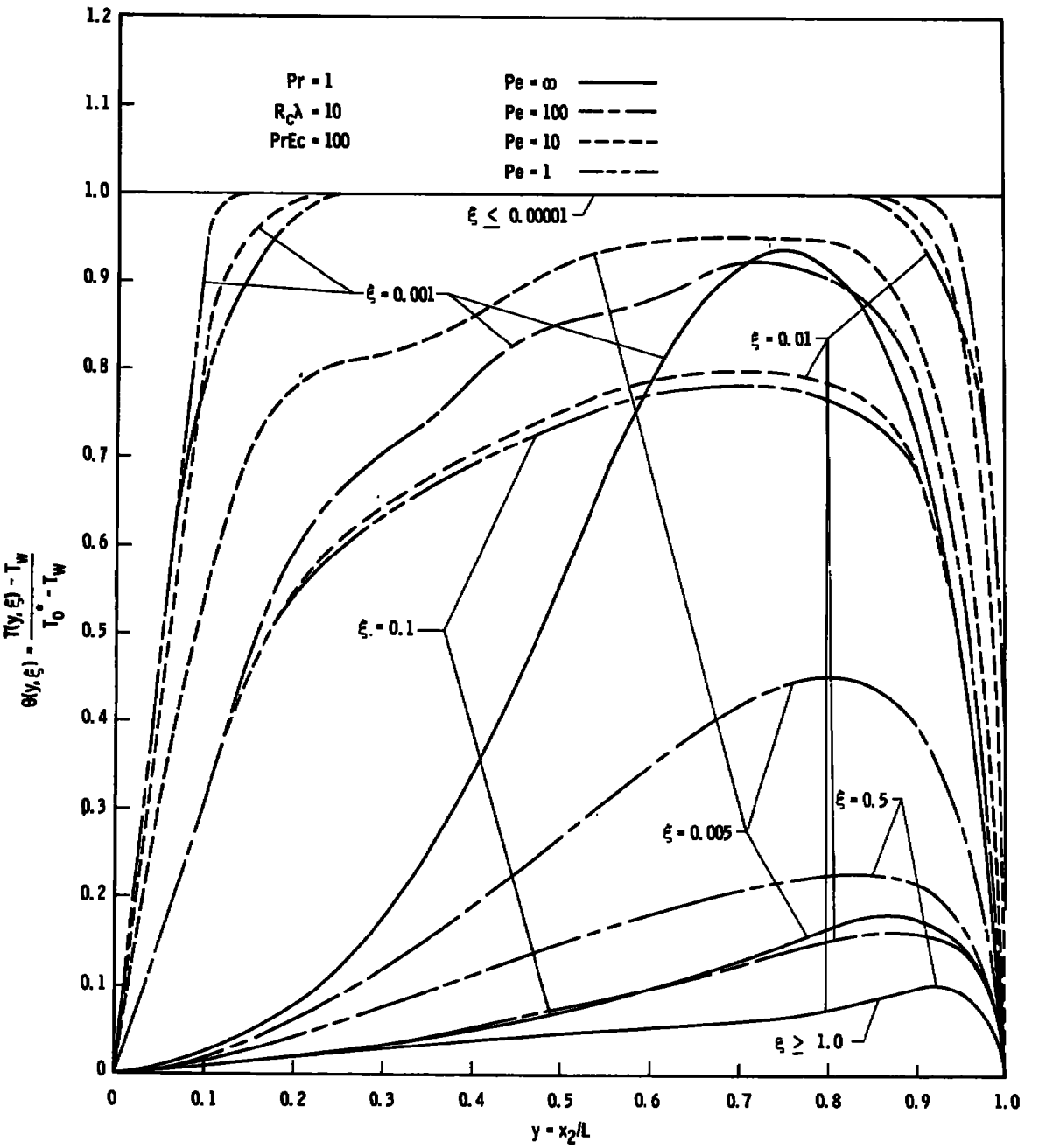

Fig. 9 Temperature Profiles; Pr = 1, $R_c\lambda$ = 10, PrEc = 100

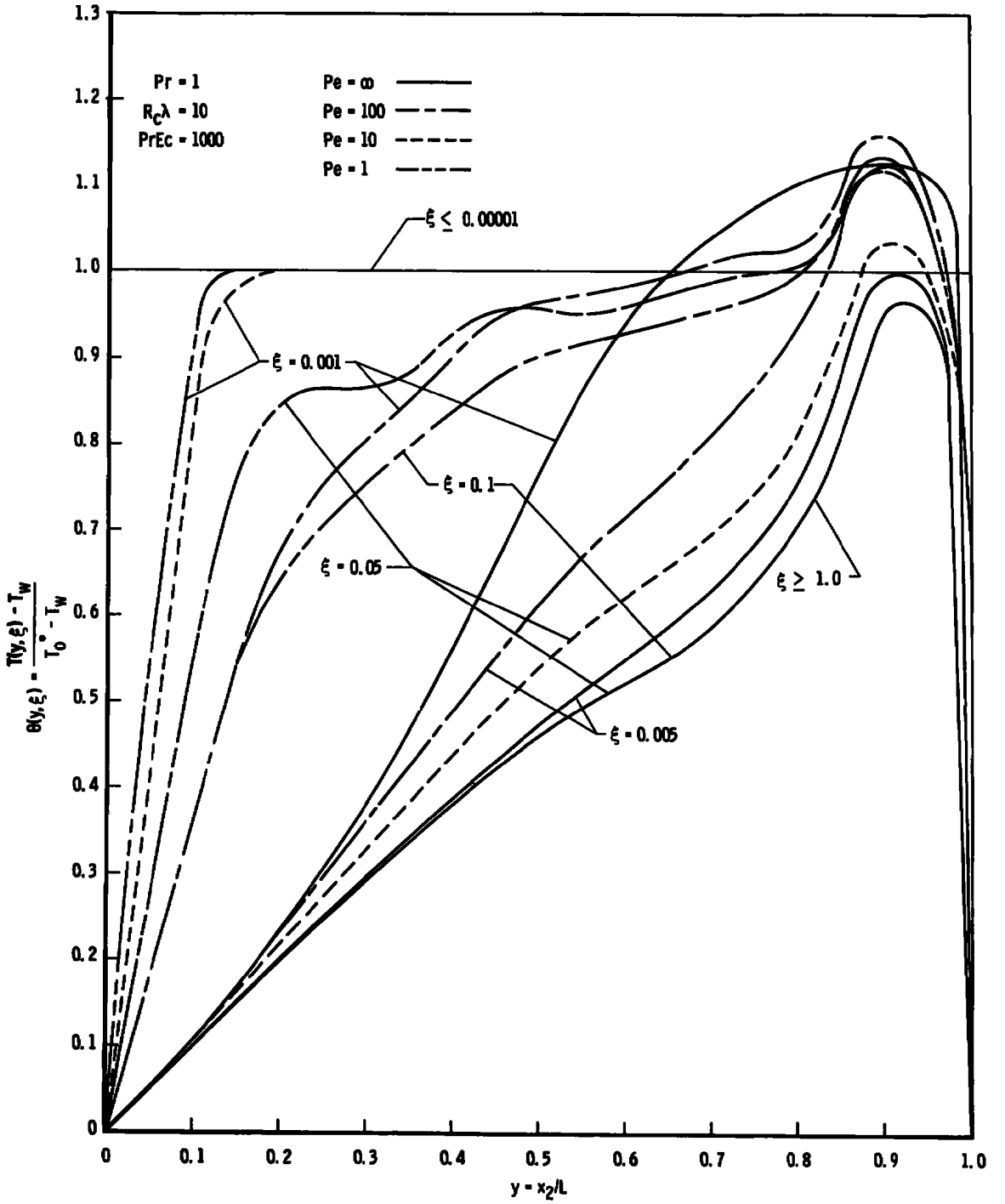

Fig. 10 Temperature Profiles; Pr = 1, $R_c\lambda$ = 10, PrEc = 1000

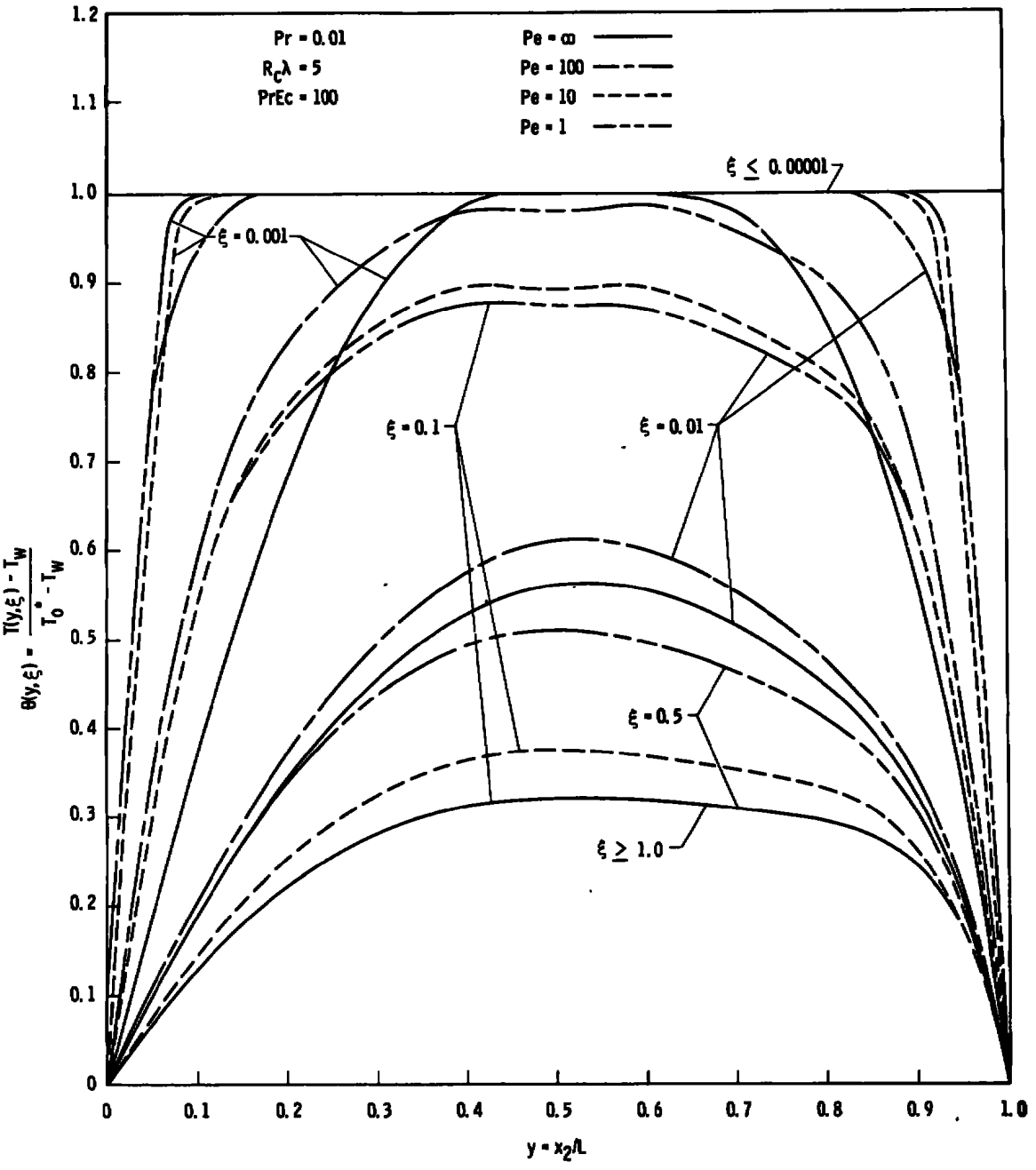

Fig. 11 Temperature Profiles; Pr = 0.01, $R_c\lambda$ = 5, PrEc = 100

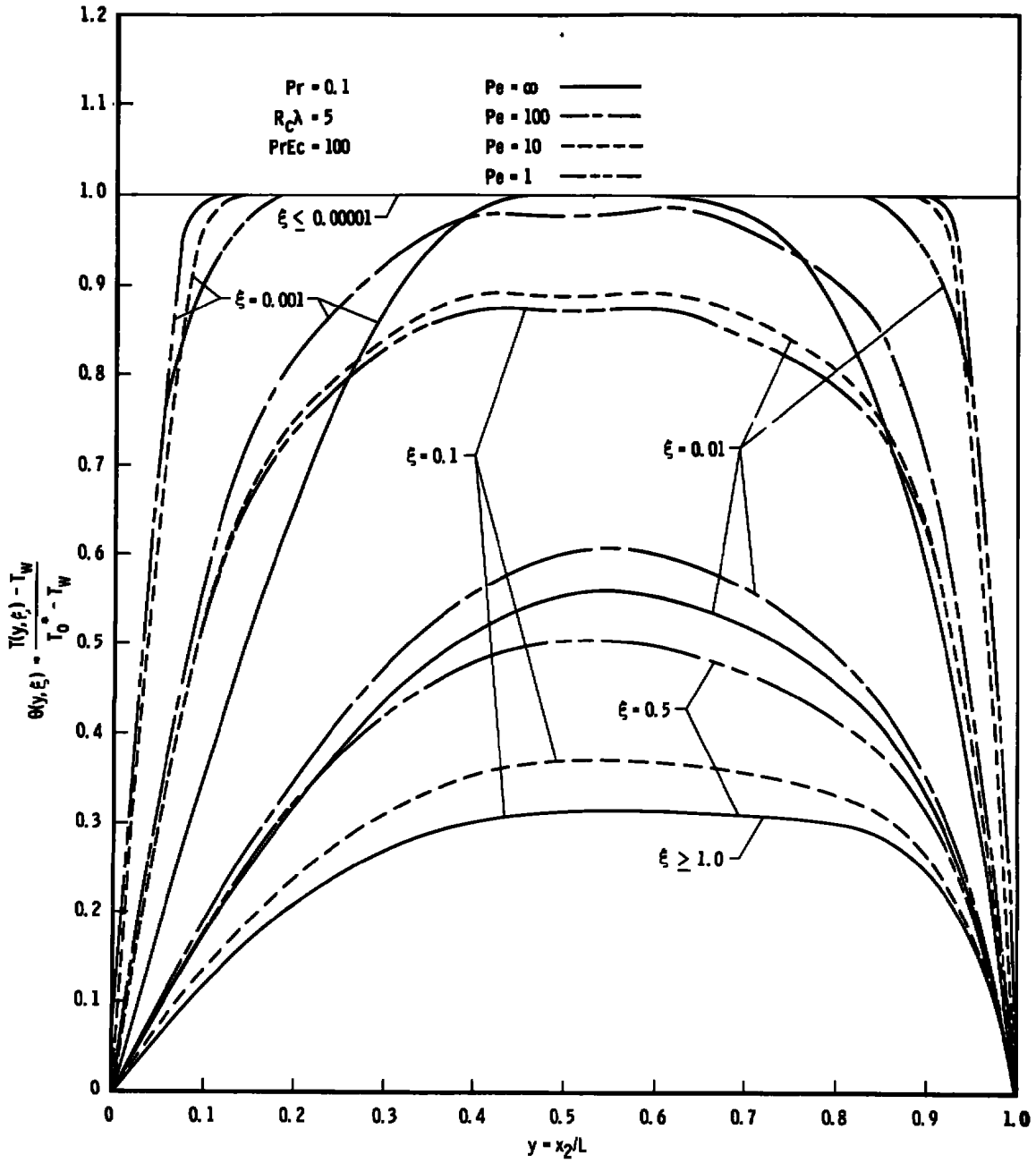

Fig. 12 Temperature Profiles; Pr = 0.1, $R_c\lambda$ = 5, PrEc = 100

of the excess temperature profiles for a particular value of ξ. This can easily be explained since increasing values of $R_c\lambda$ decrease the mean velocity of the fluid for a given pressure drop, see Figure A-2, page 74, which results in a lesser effect due to viscous dissipation.

Data are presented for three values of the product of the Prandtl and pseudo Eckert number, PrEc = 10, 100, 1000. This parameter represents the ratio of the dissipation in the fluid to conduction due to the temperature difference between the entrance and the wall conditions. In each figure PrEc = 10 represents the case of strong cooling effect due to large temperature difference between the entrance and the wall conditions, and PrEc = 1000 represents the case of dominant overall dissipation.

In the figures where the wall blowing parameter, $R_c\lambda$ = 0.1 and 1, the excess temperature profiles near the entrance region exhibit the characteristic of a dip near the channel centerline. This characteristic dip is the result of the internal heat generation due to viscous dissipation in the boundary layer region which locally creates an increase in the fluid temperature. For larger values of the wall blowing parameter, $R_c\lambda$ = 5 and 10, this characteristic dip effect is diminished due to the displacement of the velocity profile toward the upper channel wall. Figure 10, page 43, presents the case where the major portion of the viscous dissipation occurs near the upper wall of the channel.

Figures 11 and 12, pages 44 and 45, are presented to show the effect of the Prandtl number on the dimensionless excess temperature profiles. Comparing Figure 8, page 41, with Figures 11 and 12 in which

$R_c\lambda = 5$, PrEc = 100, with the Prandtl number, Pr = 0.01, 0.1, and 1, the temperature profiles are noted to become more non-symmetrical as the Prandtl number increases with the maximum temperatures being displaced toward the upper channel wall. The dimensionless excess temperature profiles presented in Figures 11 and 12, pages 44 and 45, are noted to be very similar; however, the profiles in Figure 8, page 41, when compared to the lower Prandtl numbers are seen to be considerably different. The larger value of Prandtl number, Pr = 1, is seen to have a relatively strong influence on the excess temperature distribution.

It is interesting to note that for the lower Peclet numbers, Pe = 100, 10, 1, the complete temperature profile across the channel, in a sense, lags compared to the temperature profiles at Peclet number, Pe = ∞. This effect can easily be justified by considering the fact that the strong axial conduction at low Peclet numbers results in heat transfer from the local cross section to the entrance plane, in addition to the cooling through the channel walls. Neglecting axial conduction by assuming the Peclet number infinite which is most commonly treated in the literature can introduce considerable error in the temperature profiles for values of the axial coordinate, $\xi \leq 1.0$.

CHAPTER VI
CALCULATIONS FOR THE BULK MEAN TEMPERATURE AND THE LOCAL NUSSELT NUMBER

Since the temperature profiles are not necessarily symmetric about the channel centerline, the value of the local Nusselt number based on the heat transfer through the upper wall, y = 1, and through the lower wall, y = 0, is expected to have different values. The local Nusselt numbers for each wall are defined as:

$$Nu(0,x_3) = L[T_m(x_3) - T_w]^{-1} \frac{\partial T}{\partial x_2} \quad (0,x_3) \tag{57}$$

and,

$$Nu(L,x_3) = -L[T_m(x_3) - T_w]^{-1} \frac{\partial T}{\partial x_2}(L,x_3) \tag{58}$$

where $T_m(x_3)$ is the local bulk mean temperature of the fluid,

$$T_m(x_3) = \frac{\int_0^L V_3(x_2)\, T(x_2,x_3)dx_2}{\int_0^L V_3(x_2)dx_2} \tag{59}$$

Equation 59 can be non-dimensionalized to yield a dimensionless bulk mean temperature, $\theta_m(\xi)$, as

$$\theta_m(\xi) = \frac{T_m(x_3) - T_w}{T_o^* - T_w} = \frac{\int_0^1 u(y)\theta(y,\xi)dy}{\int_0^1 u(y)dy} \tag{60}$$

The slopes of the temperature profile at each wall become,

$$\frac{\partial T}{\partial x_2}(0,x_3) = \frac{T_o^* - T_w}{L} \frac{\partial \theta}{\partial y}(0,\xi) \tag{61}$$

$$\frac{\partial T}{\partial x_2}(L,x_3) = \frac{T_o^* - T_w}{L} \frac{\partial \theta}{\partial y}(1,\xi) \tag{62}$$

Therefore the equations for the local Nusselt numbers become,

$$Nu(0,\xi) = Nu^{(0)} = Nu(0,x_3) = \frac{\frac{\partial \theta}{\partial y}(0,\xi)}{\theta_m(\xi)} \tag{63}$$

$$Nu(1,\xi) = Nu^{(1)} = Nu(1,x_3) = -\frac{\frac{\partial \theta}{\partial y}(1,\xi)}{\theta_m(\xi)} \tag{64}$$

Hence, a modified form of the local Nusselt numbers in terms of the dimensionless temperatures becomes,

$$Nu(0,\xi) = \left[\int_0^1 u(y)dy\right]\left[\frac{\partial \Omega}{\partial y}(0,\xi) + \frac{\partial \theta_\infty}{\partial y}(0)\right] \left\{\int_0^1 u(y)\,\Omega(y,\xi)dy + \int_0^1 u(y)\,\theta_\infty(y)dy\right\}^{-1} \tag{65}$$

and

$$Nu(1,\xi) = -\left[\int_0^1 u(y)dy\right]\left[\frac{\partial \Omega}{\partial y}(1,\xi) + \frac{\partial \theta_\infty}{\partial y}(1)\right] \left\{\int_0^1 u(y)\Omega(y,\xi)dy + \int_0^1 u(y)\theta_\infty(y)dy\right\}^{-1} \tag{66}$$

Since the general expressions for $\Omega(y,\xi)$ and $\theta_\infty(y)$ are already obtained, the terms in Equations 65 and 66 can be evaluated for each wall as:

$$\int_0^1 u(y)dy = \frac{1}{R_c\lambda}\left[\frac{1}{2} - \frac{1}{1 - e^{R_c\lambda}} - \frac{1}{R_c\lambda}\right] \tag{67}$$

$$\int_0^1 u(y)\Omega(y,\xi)dy = \frac{4\pi}{R_c\lambda}\sum_{n=1}^{K} A_n e^{-\beta_n\xi}\sum_{i=1}^{N} c_i(n)$$

$$\left\{\frac{-i\, e^{\frac{1}{2}PrR_c\lambda}(-1)^i}{(PrR_c\lambda)^2 + 4i^2\pi^2} + \frac{4PrR_c\lambda i\left[e^{\frac{1}{2}R_c\lambda(Pr+2)}(-1)^i - 1\right]}{\left[(PrR_c\lambda)^2 + 4i^2\pi^2\right]^2}\right.$$

$$\left.\frac{i\left[e^{\frac{1}{2}PrR_c\lambda}(-1)^i - 1\right]}{(1-e^{R_c\lambda})\left[(PrR_c\lambda)^2+4i^2\pi^2\right]} - \frac{i\left[e^{\frac{PrR_c\lambda}{2}(Pr+2)} - (1)^i - 1\right]}{(1-e^{R_c\lambda})\left[R_c{}^2\lambda^2(Pr+2)^2+4i^2\pi^2\right]}\right\} \tag{68}$$

$$\int_0^1 u(y)\theta_\infty(y)dy = \frac{4\pi PrEc}{R_c\lambda}\sum_{i=1}^{M} D_i\left\{-\frac{i\, e^{\frac{1}{2}PrR_c\lambda}(-1)^i}{(PrR_c\lambda)^2+4i^2\pi^2} + \right.$$

$$\frac{4iPrR_c\lambda\left[e^{\frac{1}{2}PrR_c\lambda}(-1)^i - 1\right]}{\left[(PrR_c\lambda)^2 + 4i^2\pi^2\right]^2} + \frac{i\left[e^{\frac{1}{2}PrR_c\lambda}(-1)^i - 1\right]}{(1-e^{R_c\lambda})\left[(PrR_c\lambda)^2+4i^2\pi^2\right]} -$$

$$\left.\frac{i\, e^{\left[\frac{R_c\lambda}{2}(Pr+2)\right]}(-1)^i - 1}{(1-e^{R_c\lambda})\left[R_c{}^2\lambda^2(Pr+2)^2+4i^2\pi^2\right]}\right\} \tag{69}$$

$$\frac{\partial\Omega}{\partial y}(1,\xi) = \sum_{n=1}^{K} A_n e^{-\beta_n\xi}\sum_{i=1}^{N} c_i(n)\, e^{\frac{1}{2}PrR_c\lambda}\, i\pi(-1)^i \tag{70}$$

$$\frac{\partial\theta_\infty}{\partial y}(1) = PrEc\, e^{\frac{1}{2}PrR_c\lambda}\sum_{i=1}^{M} D_i\, i\pi\,(-1)^i \tag{71}$$

$$\frac{\partial \Omega}{\partial y}(0,\xi) = \sum_{n=1}^{K} A_n e^{-\beta_n \xi} \sum_{i=1}^{N} c_i^{(n)} i\pi \tag{72}$$

$$\frac{\partial \theta_\infty}{\partial y}(0) = PrEc \sum_{i=1}^{M} D_i i\pi \tag{73}$$

An average Nusselt number, $\overline{Nu}(x_3)$, based on the net heat transfer from the system can be defined as,

$$\overline{Nu}(x_3) = \frac{QL}{\kappa A(T_m - T_w)} \tag{74}$$

where A is the total surface area of the system. The average Nusselt number based on the previously defined Nusselt numbers for each wall becomes,

$$\overline{Nu}(\xi) = \overline{Nu}(x_3) = \frac{Nu(0,\xi) + Nu(L,\xi)}{2} \tag{75}$$

The dimensionless bulk mean temperature and the local Nusselt number for wall blowing parameter, $R_c = 0.1$, Prandtl number, Pr = 1, Peclet number, Pe = ∞, and product of the Prandtl number and pseudo Eckert number, PrEc = 0, are plotted in Figures 13 and 14. These conditions represent closely the hydrodynamic case which neglects effects of wall blowing, viscous dissipation and axial conduction. These data are in good agreement with those found in Reference 2 which are also plotted in Figures 13 and 14. The agreement of the present data with those found in Reference 2 indicates confidence in the data reduction procedure

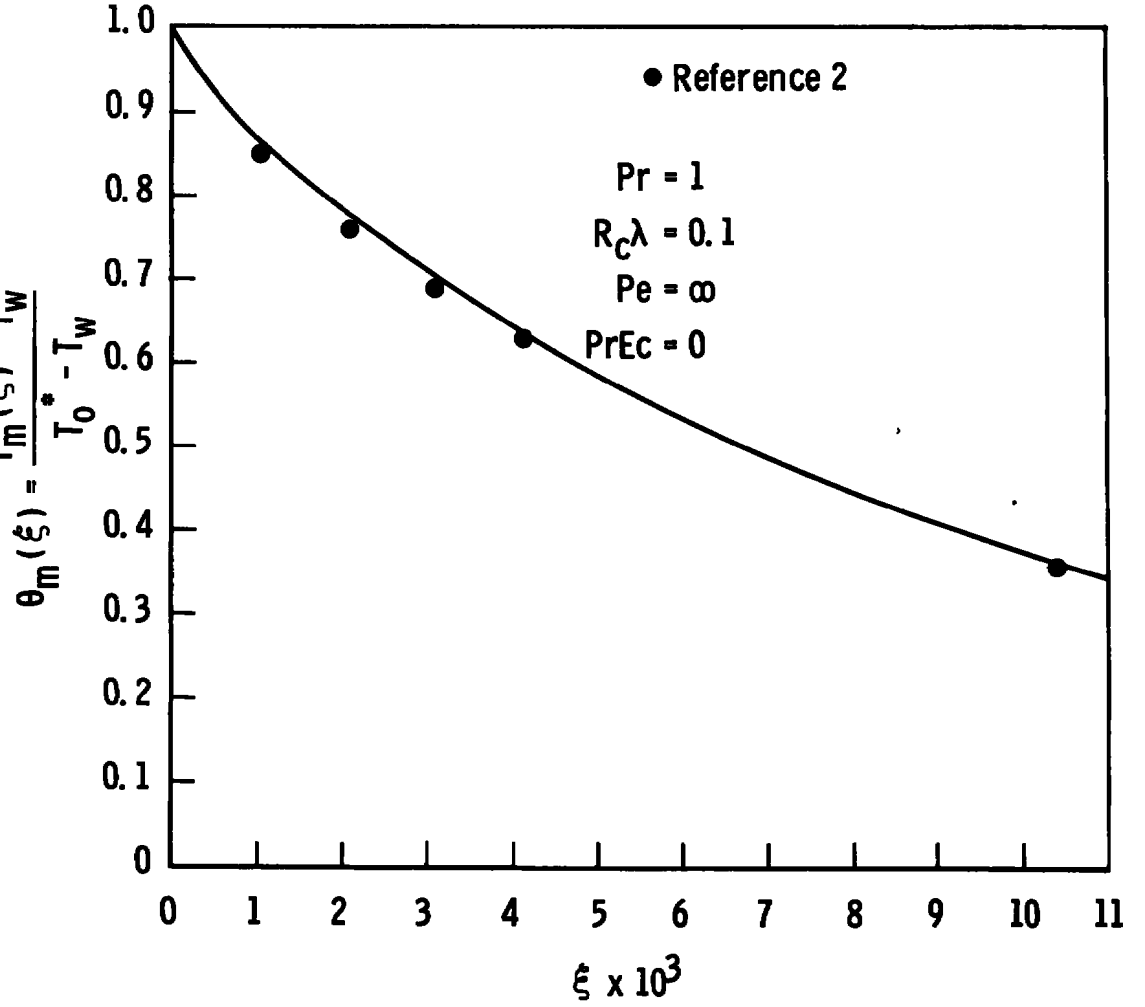

Fig. 13 Bulk Temperature Assuming No Viscous Dissipation or Axial Conduction

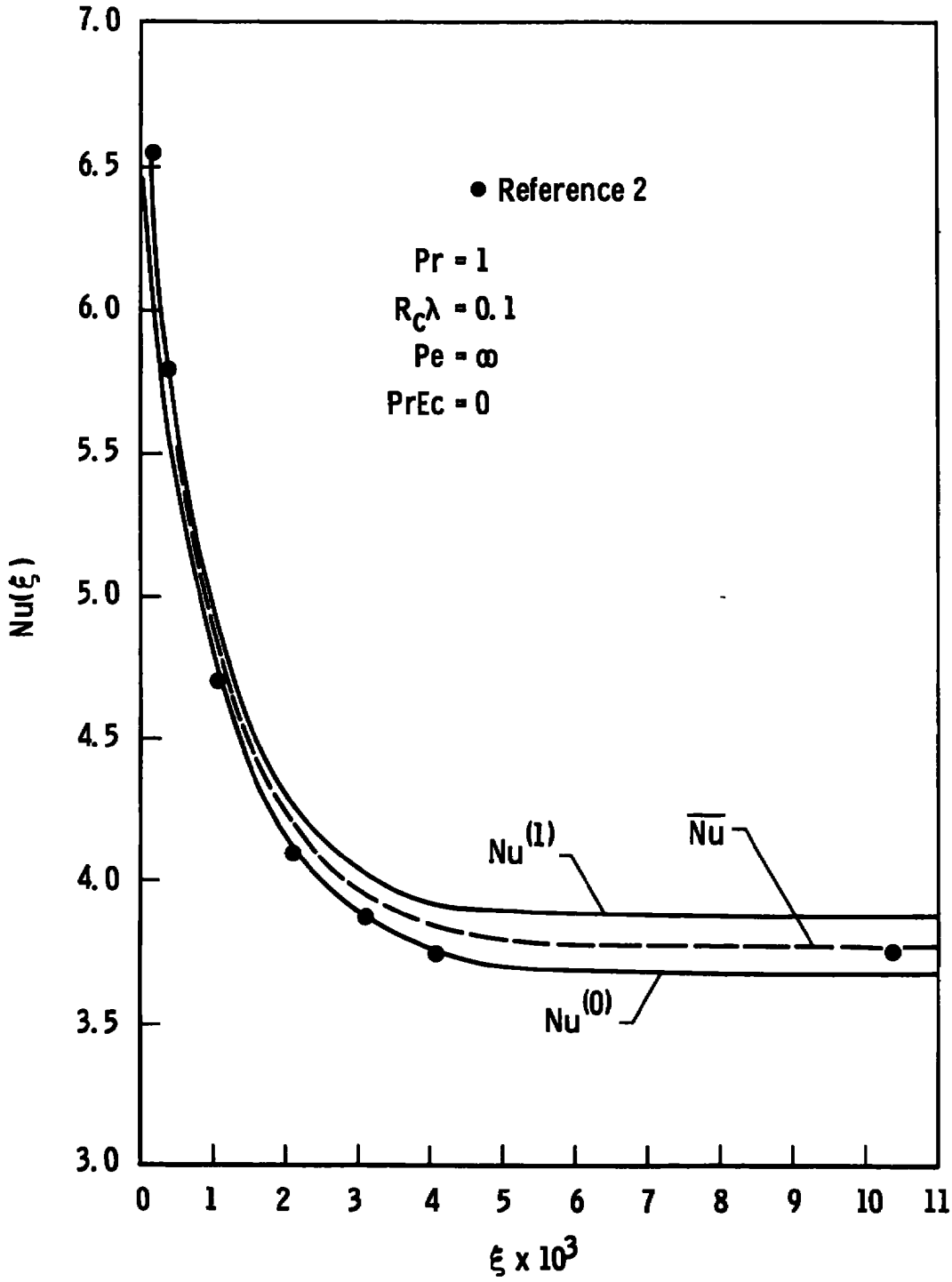

Fig. 14 Local Nusselt Number Assuming No Viscous Dissipation or Axial Conduction

used in this study.

The development along the axial direction, ξ, of the dimensionless bulk mean temperature, $\theta_m(\xi)$, and the local Nusselt numbers, $Nu(1,\xi)$, and $Nu(0,\xi)$, for the upper and lower channel wall and the average Nusselt number, $\overline{Nu}(\xi)$, are presented in Figures 15 through 24 for various values of wall blowing parameter, $R_c\lambda$, Prandtl number, Pr, Peclet number, Pe, and the product of the Prandtl number and pseudo Eckert number, PrEc.

The effect of the wall blowing parameter on the dimensionless bulk mean temperature is shown in Figures 15a through 18a for Prandtl number, Pr = 1. It is noted that there is little change in the dimensionless bulk mean temperature development as the wall blowing parameter changes from 0.1 to 1; however, the larger values of wall blowing parameter, $R_c\lambda$ = 5 and 10, tend to decrease the magnitude of the bulk mean temperature for a particular value of ξ. As in the discussion of the temperature profiles, this effect can be explained since increasing values of $R_c\lambda$ decrease the mean velocity of the fluid for a given pressure drop which results in a lesser effect due to viscous dissipation.

Inspection of the bulk mean temperatures presented in Figures 17a, 19a, and 21a for wall blowing parameter, $R_c\lambda$ = 5, and Prandtl number, Pr = 0.01, 0.1, and 1, indicates relatively small effect due to changes in the Prandtl number. It can be shown that the fully developed bulk mean temperature for the hydrodynamic case with no wall blowing is

$$\frac{T_m - T_w}{T_o^* - T_w} = 0.00476\ PrEc \tag{76}$$

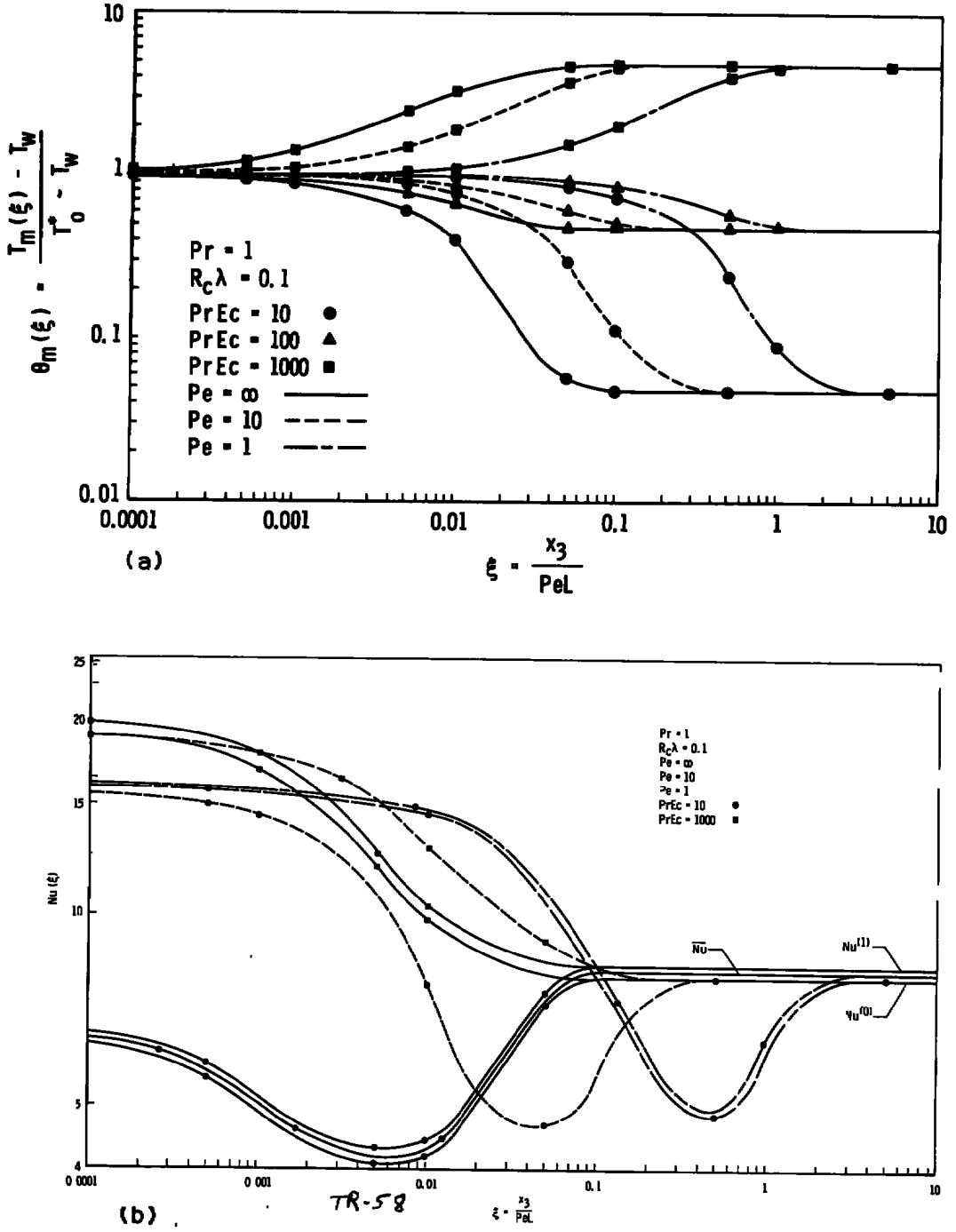

Fig. 15 Heat Transfer Parameters; Pr = 1, $R_c\lambda$ = 0.1

(a) Bulk Mean Temperature; (b) Local Nusselt Number

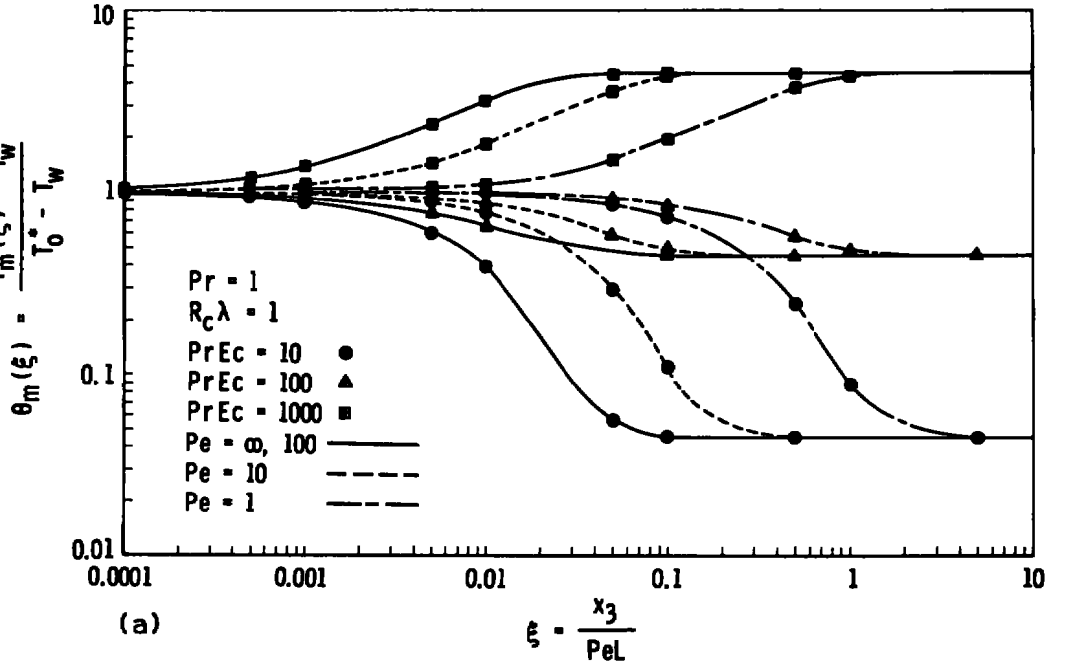

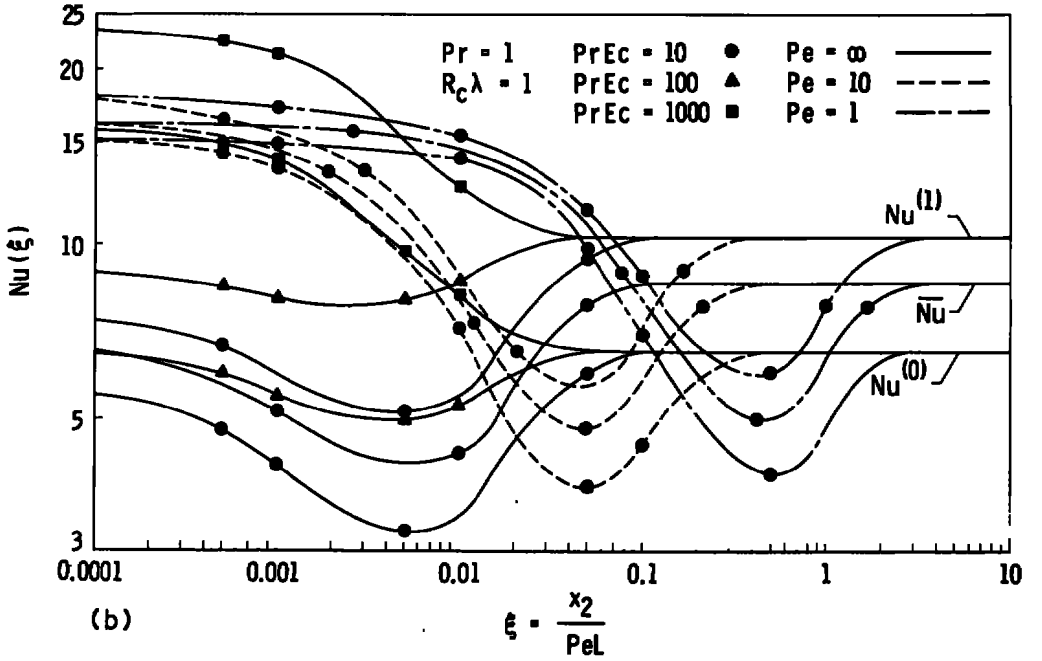

Fig. 16 Heat Transfer Parameters; Pr = 1, $R_c\lambda$ = 1

(a) Bulk Mean Temperature; (b) Local Nusselt Number

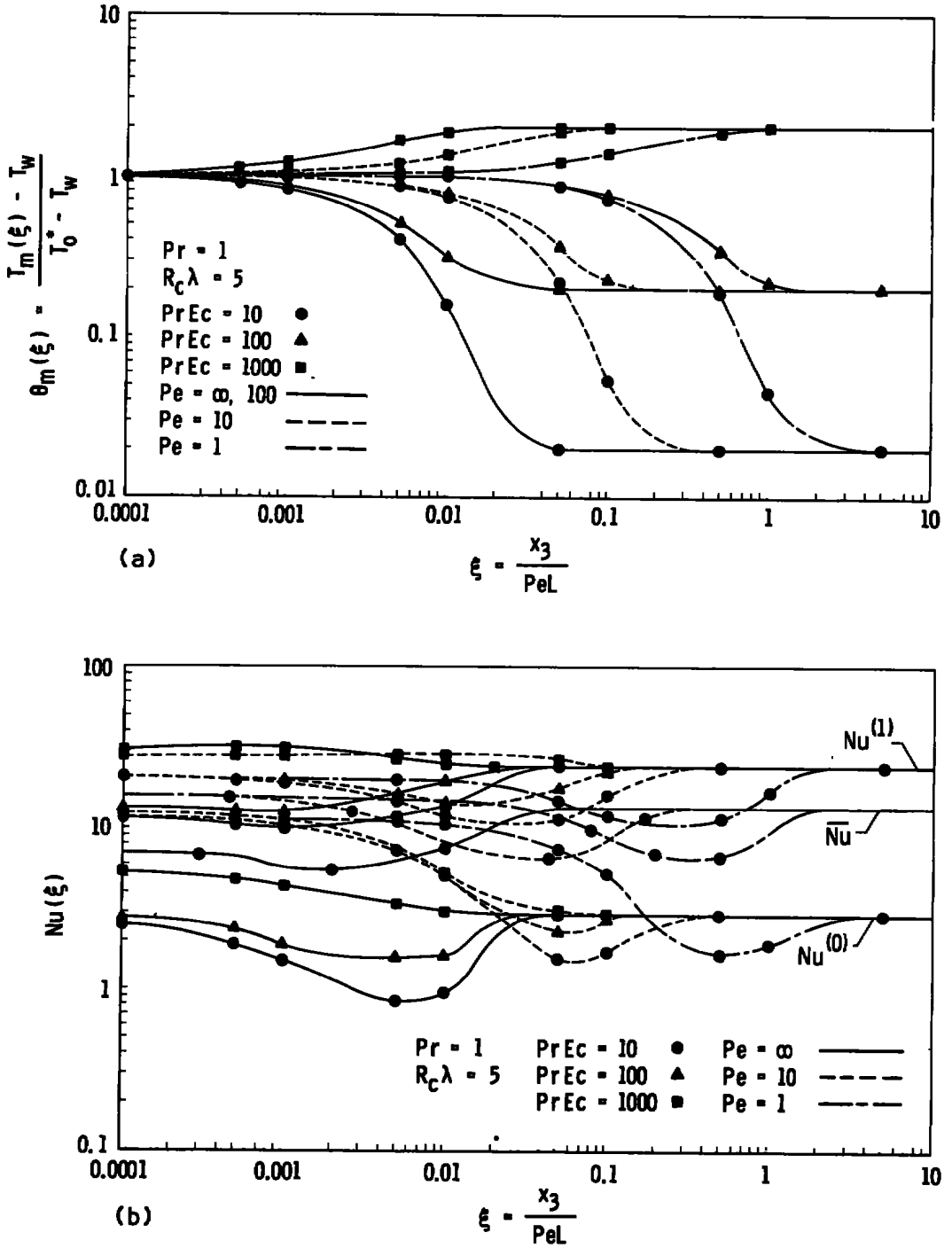

Fig. 17 Heat Transfer Parameters; Pr = 1, $R_c\lambda$ = 5

(a) Bulk Mean Temperature; (b) Local Nusselt Number

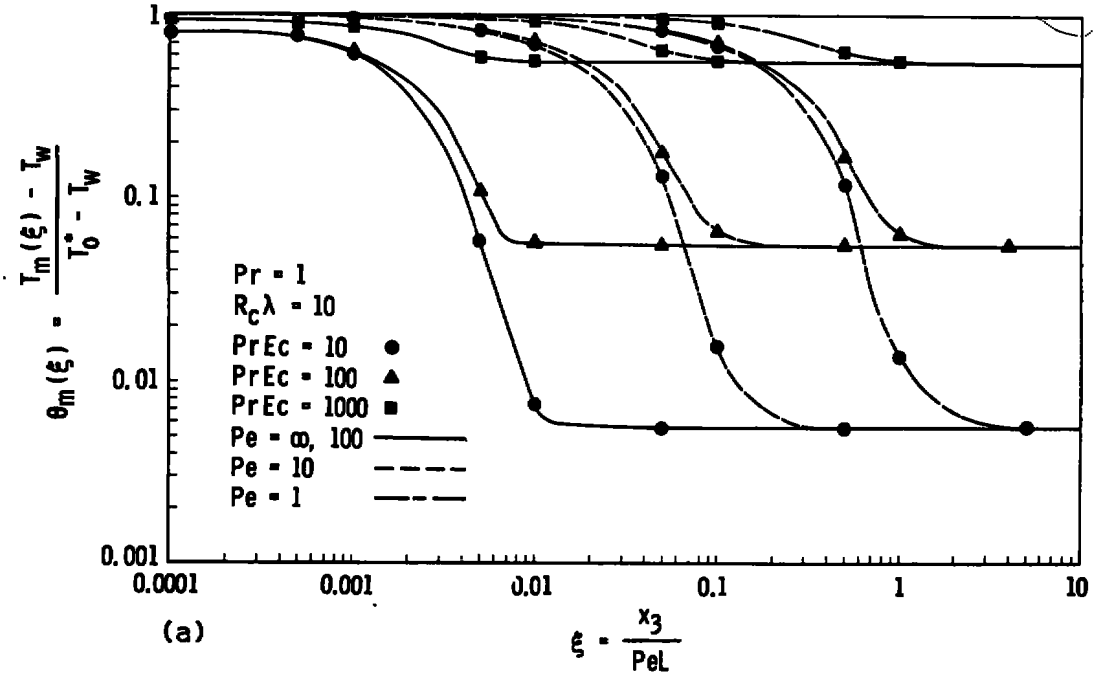

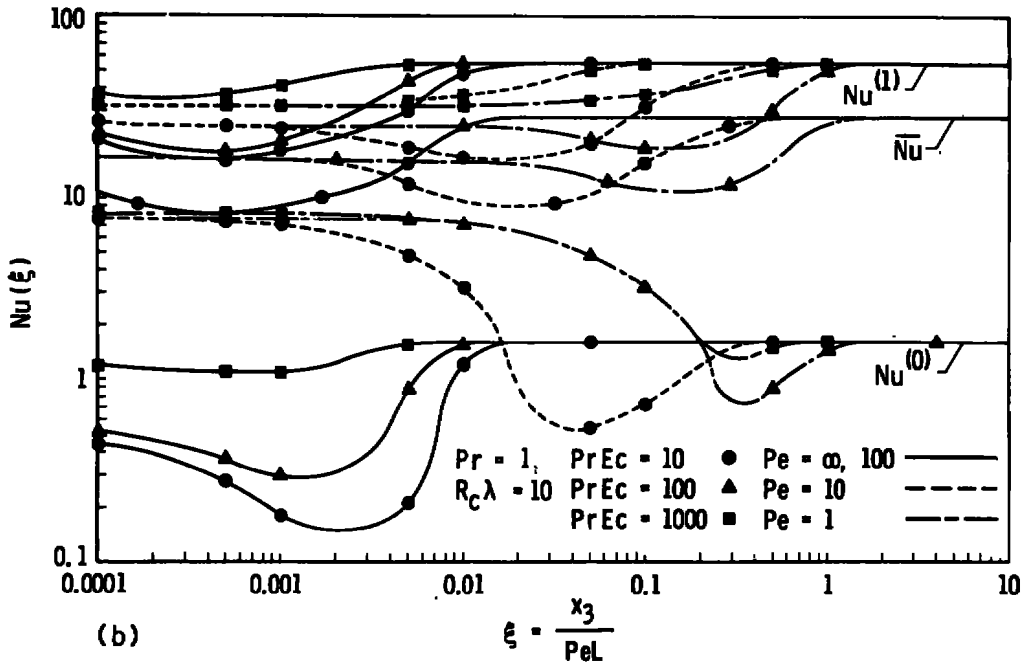

Fig. 18 Heat Transfer Parameters; Pr = 1, $R_c\lambda$ = 10

(a) Bulk Mean Temperature; (b) Local Nusselt Number

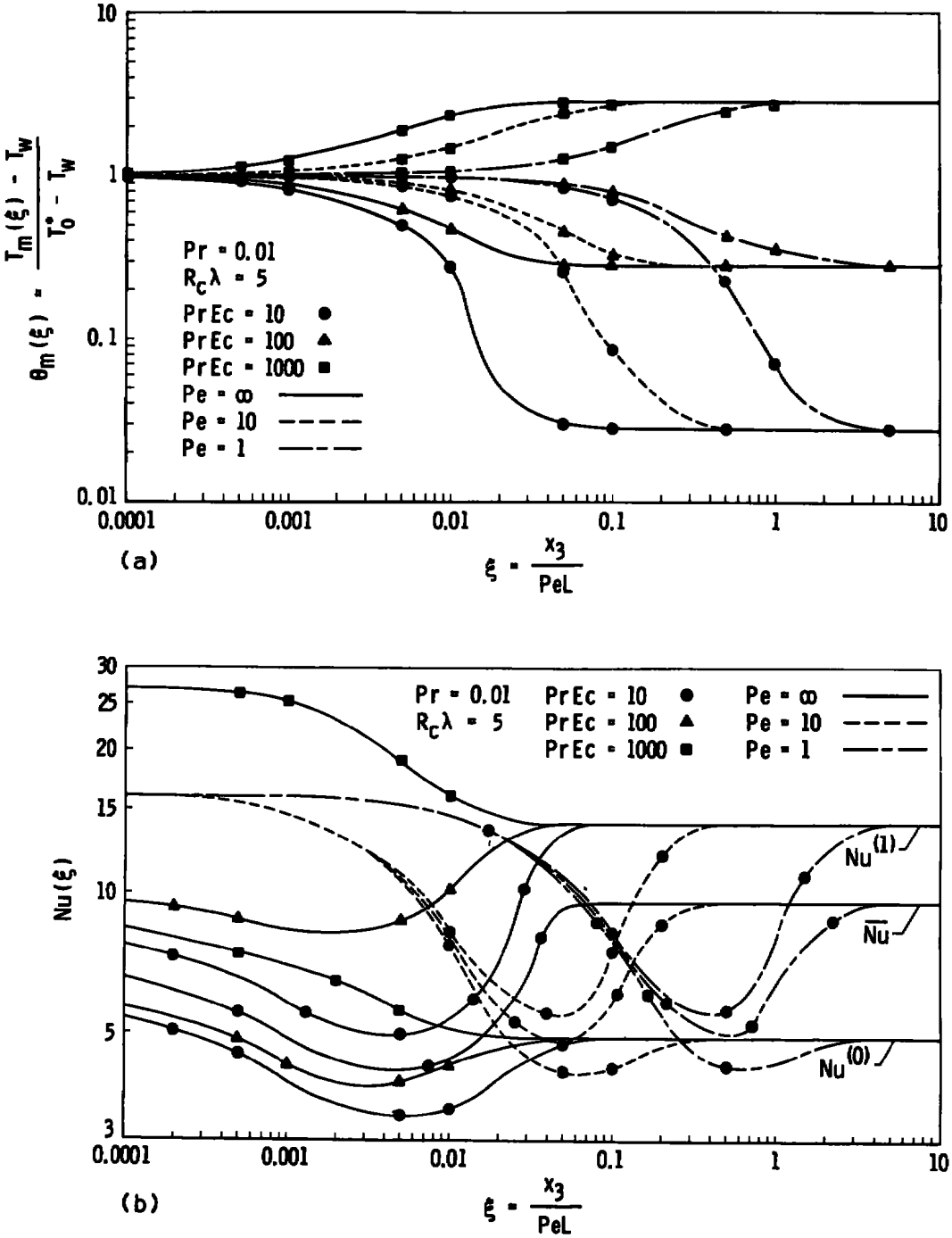

Fig. 19 Heat Transfer Parameters; Pr = 0.01, $R_c\lambda$ = 5

(a) Bulk Mean Temperature; (b) Local Nusselt Number

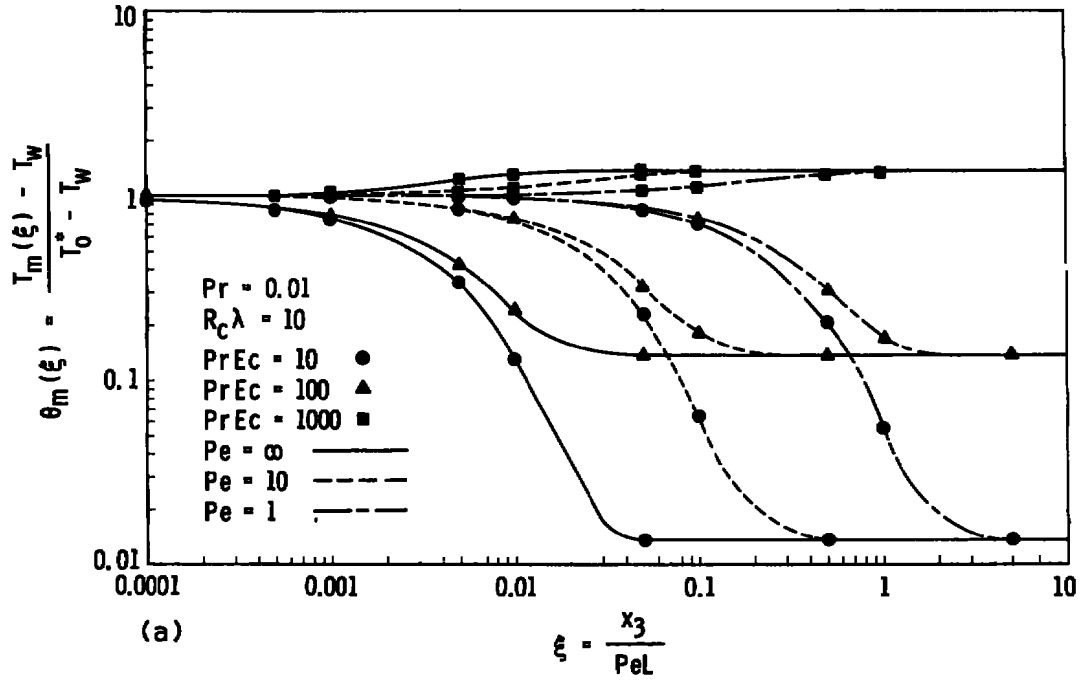

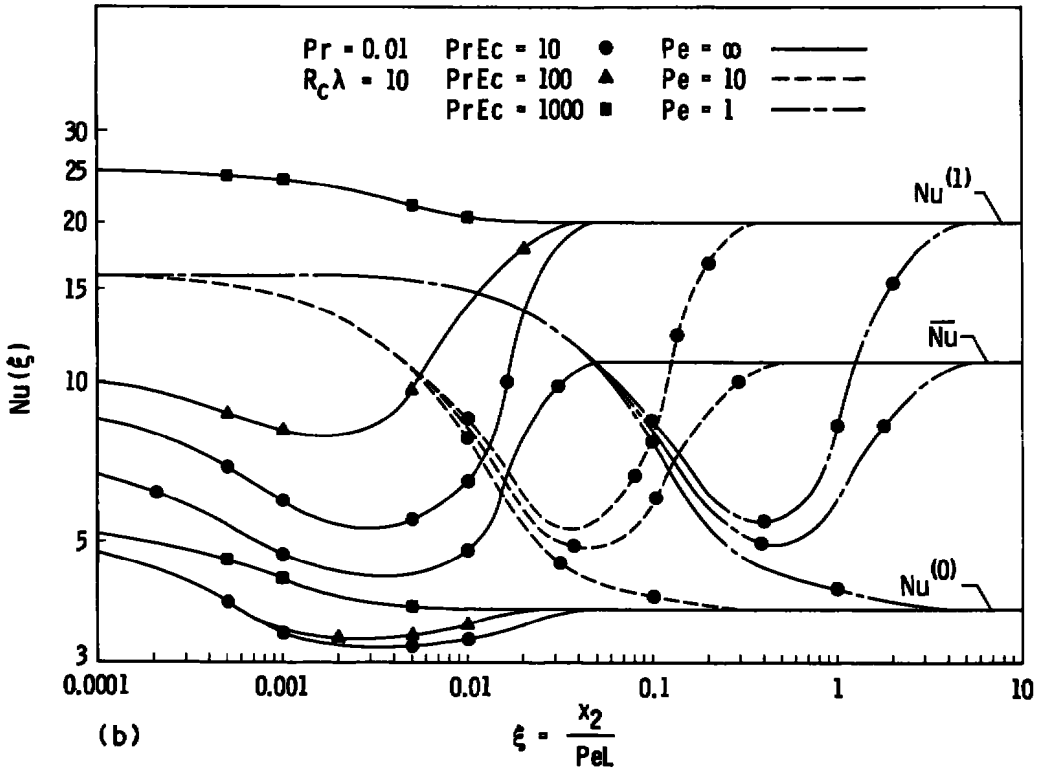

Fig. 20 Heat Transfer Parameters; Pr = 0.01, $R_c\lambda$ = 10

(a) Bulk Mean Temperature; (b) Local Nusselt Number

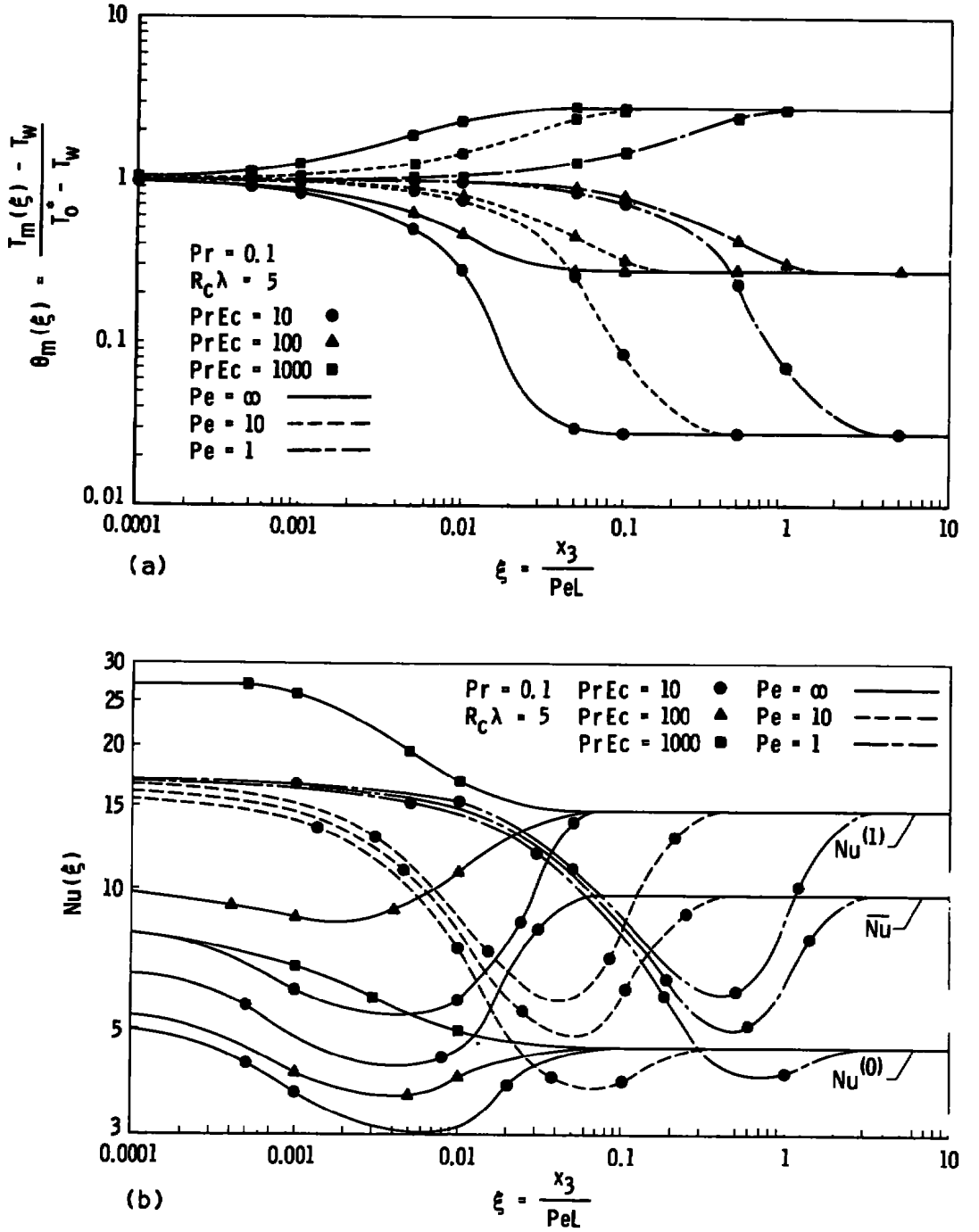

Fig. 21 Heat Transfer Parameters; Pr = 0.01, $R_c\lambda$ = 5

(a) Bulk Mean Temperature; (b) Local Nusselt Number

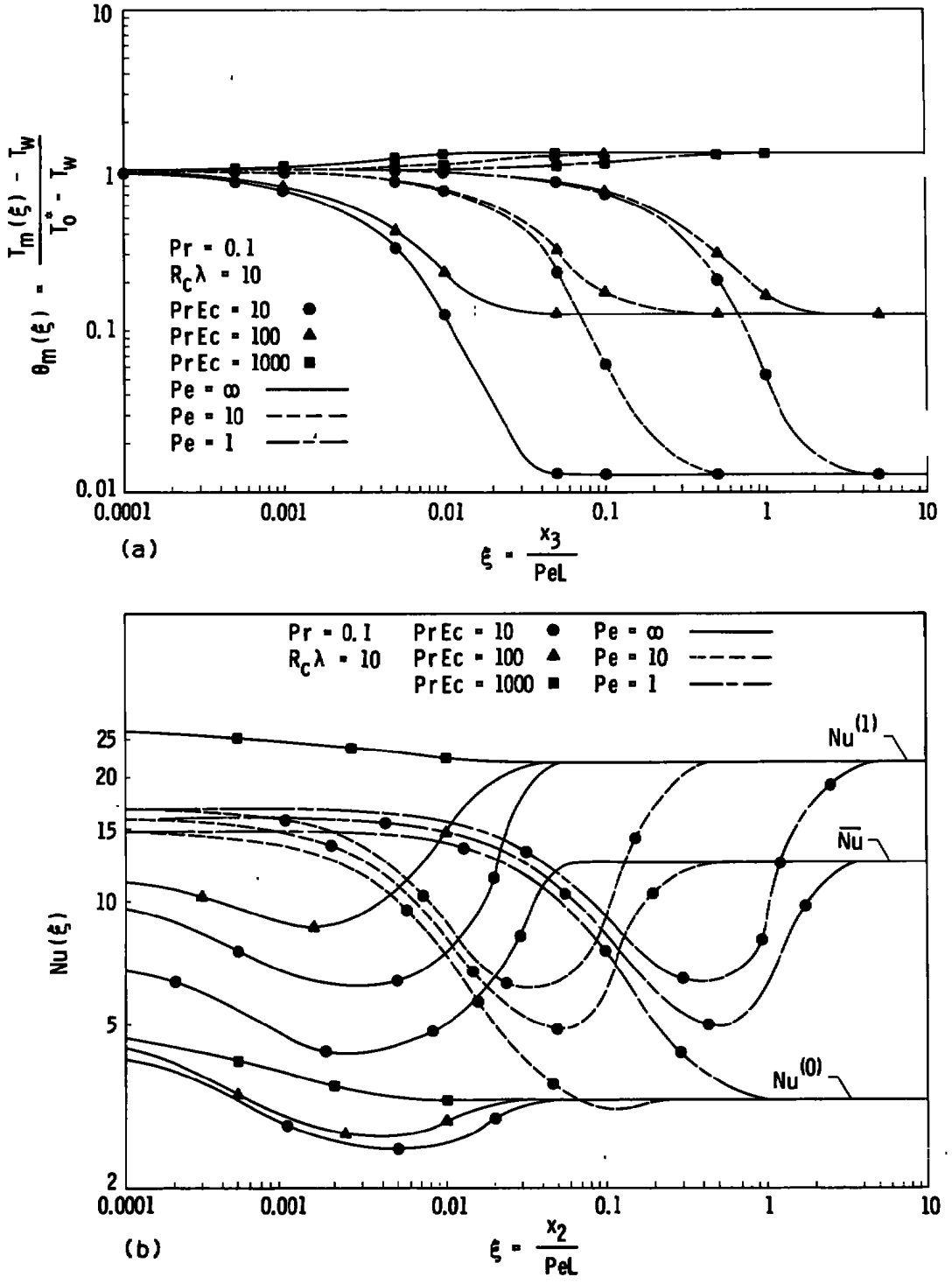

Fig. 22 Heat Transfer Parameters; Pr = 0.1, $R_c\lambda$ = 10

(a) Bulk Mean Temperature; (b) Local Nusselt Number

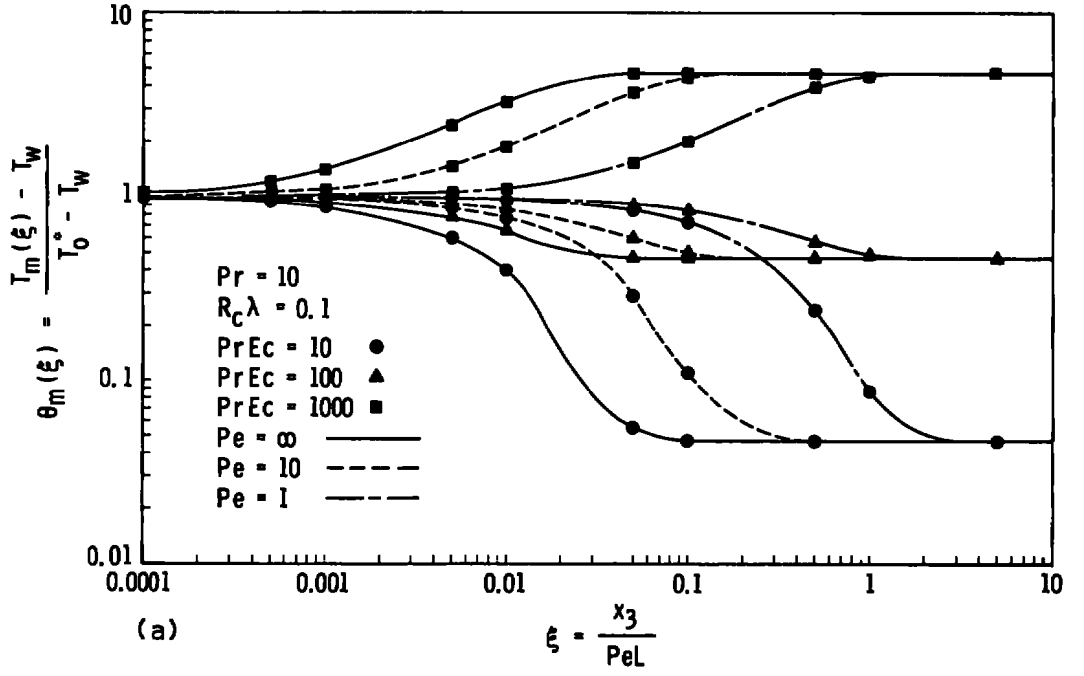

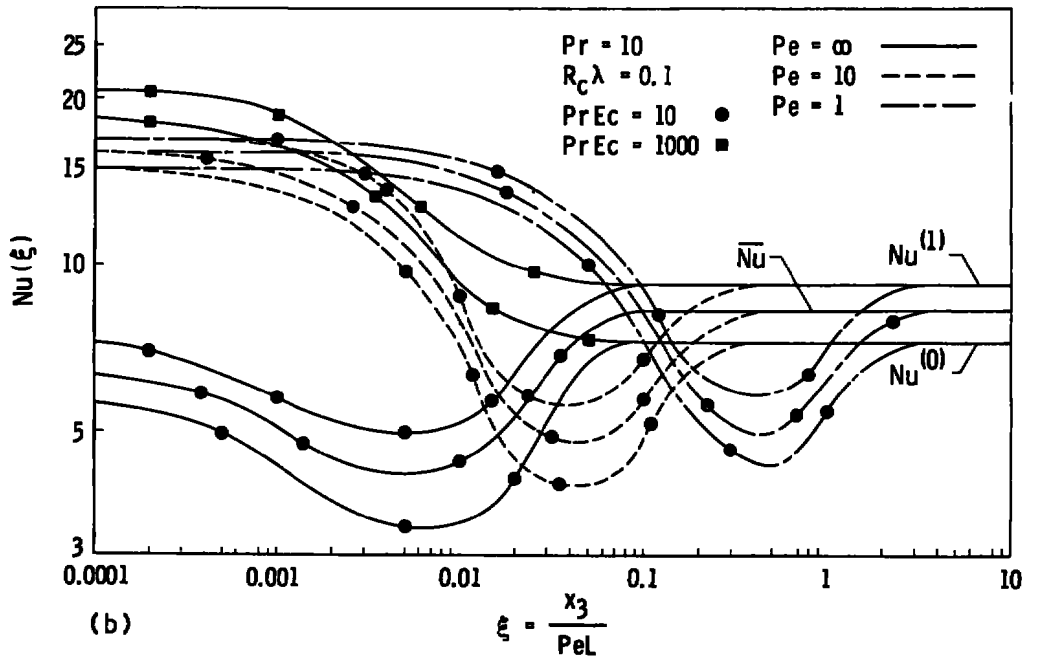

Fig. 23 Heat Transfer Parameters; Pr = 10, $R_c\lambda$ = 0.1

(a) Bulk Mean Temperature; (b) Local Nusselt Number

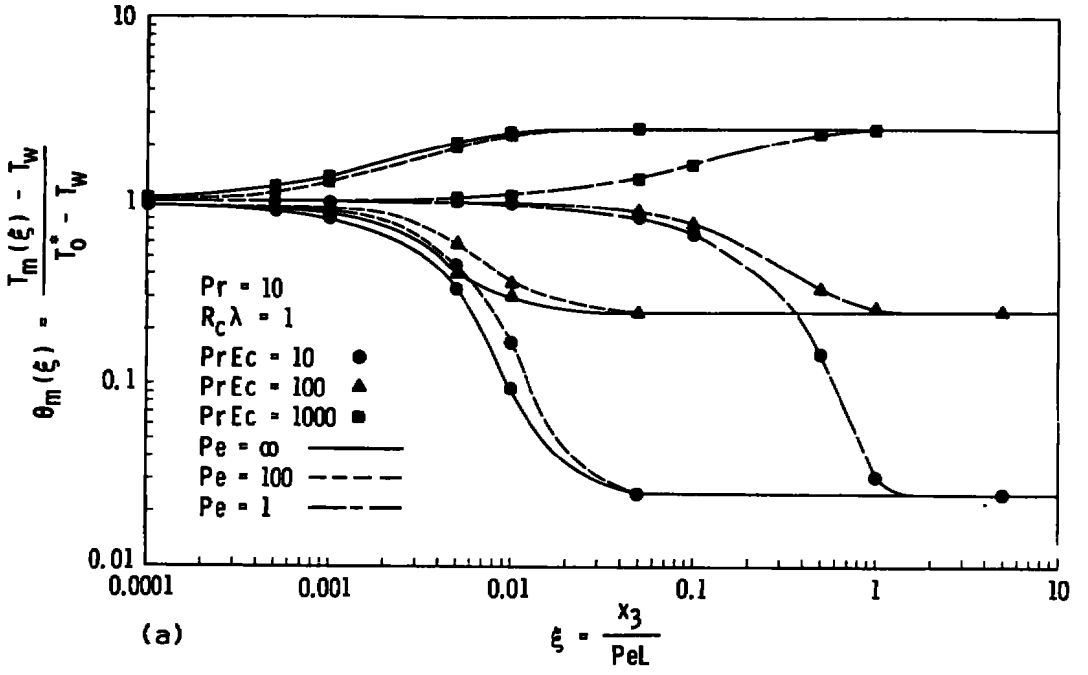

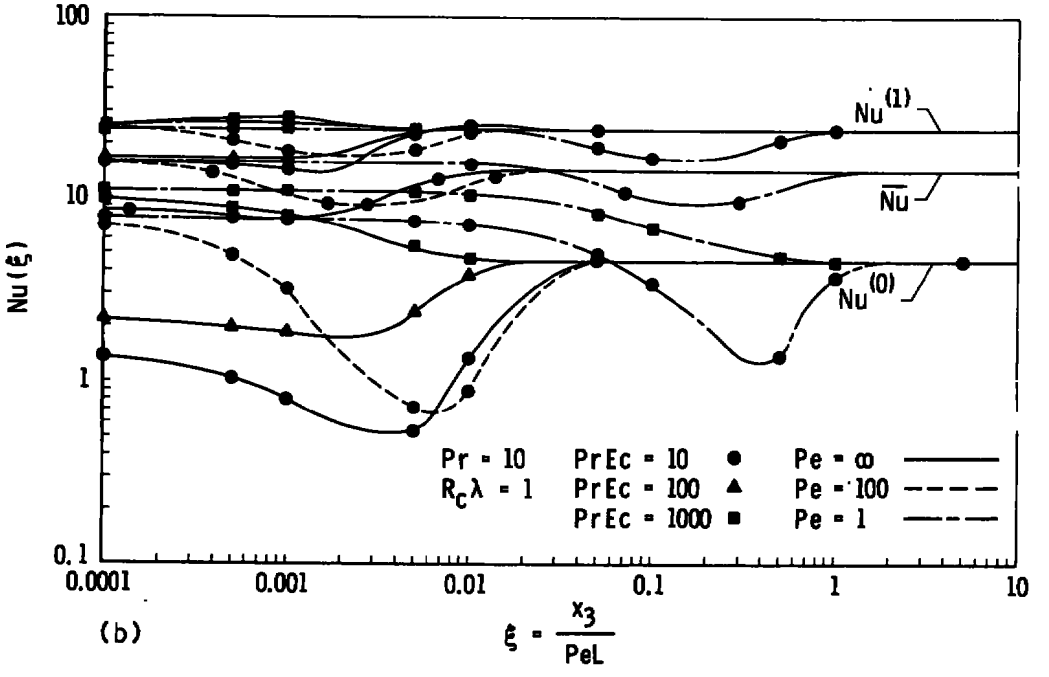

Fig. 24 Heat Transfer Parameters; Pr = 10, $R_c\lambda$ = 1

(a) Bulk Mean Temperature; (b) Local Nusselt Number

Equation 76 is in excellent agreement with the fully developed bulk mean temperatures found in Figure 15a, page 55, for Prandtl number, Pr = 1, and wall blowing parameter, $R_c\lambda = 0.1$, which approximates closely the no wall blowing case.

Figures 15b through 18b, pages 55 through 58, with Prandtl number, Pr = 1, demonstrate the effect of the wall blowing parameter, $R_c\lambda$, on the development of the local Nusselt numbers. As was expected from observation of the temperature profiles, the lower wall Nusselt number, $Nu^{(0)}$, is decreased and the upper wall Nusselt number, $Nu^{(1)}$, is increased as the wall blowing parameter increases from 0.1 to 10. From Figure 18b in which $R_c\lambda = 10$, the upper wall Nusselt number is noted to be approximately 55 while the lower wall Nusselt number is noted to be approximately 1.5 for the fully developed thermal conditions. Similar differences in magnitude of the Nusselt number are noted for axial positions, ξ, where the thermal profiles are not fully developed.

It can be easily shown that the hydrodynamic case with no wall blowing has an average Nusselt number, $\overline{Nu} = 8.75$, for fully developed thermal conditions. The data presented in Figure 15b with Pr = 1 and $R_c\lambda = 0.1$ approximate the case with no wall blowing, and the Nusselt number at fully developed conditions agrees reasonably well with this value.

Inspection of the data presented in Figures 15 through 18 indicates the effect of the wall blowing parameter $R_c\lambda$, on the length of channel, ξ, required to obtain fully developed thermal conditions. It is seen that increasing values of the wall blowing parameter tend to decrease

the value of the axial coordinate, ξ, required to produce fully developed bulk mean temperatures and Nusselt numbers.

It is noted from the inspection of the curves for local Nusselt number versus axial coordinate, ξ, that a decrease in value below that for fully developed conditions exists for the product of Prandtl number and pseudo Eckert number, PrEc = 10 and 100. This dip effect in the Nusselt number indicates that the temperature slope at the channel walls is decreasing at a more rapid rate than the decrease in the bulk mean temperature. This result is due to the large temperature difference between the entrance plane and the wall conditions for the lower values of the PrEc product. For small values of axial coordinate, ξ, there is a large temperature gradient localized near the channel walls due to conductive heat transfer to the walls. In Figure 14, page 53, for the case with no viscous dissipation effects, the Nusselt number is noted to exhibit a monotonically decreasing characteristic in the thermal entrance region.

The effect of the Peclet number on the bulk mean temperature development is similar to that mentioned in the previous chapter concerning the dimensionless temperature profile development. It is seen that for the low Peclet numbers, Pe = 10 and 1, the attainment of fully developed conditions lags as compared to the case of Peclet number, Pe = ∞. Inspection of the data for the local Nusselt number reveals a similar lag in development for the low Peclet number which again verifies the importance of the axial conduction term which is usually neglected in thermal entrance region problems.

CHAPTER VII
GENERAL CONCLUSIONS

From the results of the present study, it is concluded that mathematically the B. G. Galerkin method has distinct computational advantages over the classical analytical and numerical techniques in application to the eigenvalue problems associated with thermal entrance region analyses. The complete generality of the method, pertaining to the form of the differential equation and the boundary conditions, makes it possible to obtain solutions for the extended eigenvalue systems resulting from the formulation of the problem by considering the effects of the wall blowing parameter and the axial conduction term. From this solution, expressions for the temperature distribution, bulk mean temperature, and local Nusselt numbers have been obtained.

Numerical results have been presented to show the effects of the wall blowing parameter, viscous dissipation, and axial conduction on the temperature and local Nusselt number development in the entrance region of a parallel plate channel under constant temperature wall conditions. The results verify the fact that for small Peclet numbers the temperature profiles and local Nusselt numbers deviate considerably from the previously treated cases of infinite Peclet number. The data presented also indicate the marked effect of the wall blowing parameter on the temperature profiles and the heat transfer parameters.

BIBLIOGRAPHY

1. Graetz, L. "Ueber die Warmeleitungsfahigkeit von Flussigkeiten," Annalen der Physik und Chemie, 25:337-357, 1885.

2. Prins, J. A., J. Mulder, and J. Schenk. "Heat Transfer in Laminar Flow Between Parallel Plates," Applied Scientific Research, 2:431-440, 1950.

3. van der Does de Bye, J. A. W. and J. Schenk. "Heat Transfer in Laminar Flow Between Parallel Plates," Applied Scientific Research, 3:308-314, 1952.

4. Schenk, J. and H. L. Beckers. "Heat Transfer in Laminar Flow Between Parallel Plates," Applied Scientific Research, 4:405-411, 1954.

5. Cess, R. D. and E. C. Schaffer. "Heat Transfer to Laminar Flow Between Parallel Plates with a Prescribed Wall Heat Flux," Applied Scientific Research, 8:339-345, 1959.

6. Cess, R. D. and E. C. Schaffer. "Laminar Heat Transfer Between Parallel Plates with an Unsymmetrically Prescribed Heat Flux at the Walls," Applied Scientific Research, 9:64-70, 1959.

7. Poppendiek, H. F. "Forced Convection Heat Transfer in the Thermal Entrance Regions, Part I," Oak Ridge National Laboratory ORNL-913, Oak Ridge, Tennessee, March, 1951.

8. Hwang, Ching-Lai, P. J. Knieper and Liang-Tseng Fan. "Effects of Viscous Dissipation on Heat Transfer Parameters for Flow Between Parallel Plates," Journal of Applied Mathematics and Physics (ZAMP), 16:599-610, 1965.

9. Abramowitz, M. "On the Solution of the Differential Equation Occurring in the Problem of Heat Convection in Laminar Flow Through a Tube," Journal of Mathematics and Physics, 32:184-187, 1953.

10. Sellars, J. R., M. Tribus, and J. W. Klein. "Heat Transfer to Laminar Flow in a Round Tube or Flat Conduit - The Graetz Problem Extended," Journal of Heat Transfer, 78:441-448, 1956.

11. Sparrow, E. M. and R. Siegel. "Application of Variational Methods to the Thermal Entrance Region of Ducts," International Journal of Heat and Mass Transfer, 1:161-172, 1960.

12. Kays, W. M. "Numerical Solutions for Laminar Flow Heat Transfer in Circular Tubes," Journal of Heat Transfer, 151:1265-1274, 1955.

13. Hsu, Chia-Jung. "An Exact Mathematical Solution for Entrance - Region Laminar Heat Transfer with Axial Conduction," Applied Scientific Research, 17:359-376, 1967.

14. Agrawal, H. C. "Heat Transfer in Laminar Flow Between Parallel Plates at Small Peclet Numbers," Applied Scientific Research, 9:177-189, 1959.

15. LeCroy, R. C. "Temperature Development in the Entrance Region of a MHD Parallel Plate Channel," Masters thesis, University of Tennessee, Knoxville, Tennessee, June, 1967.

16. Kantorovich, L. V. and V. I. Krylov. Approximate Methods of Higher Analysis. New York: Interscience Publishers, Inc., 1958.

17. Courant, R. and D. Hibbert. Methods of Mathematical Physics. New York: Interscience Publishers, Inc., 1953.

APPENDIX A
SOLUTION FOR THE FULLY DEVELOPED VELOCITY PROFILE

The governing equation for the fully developed velocity profile is a non-homogeneous linear differential equation as follows from Equation 13,

$$\frac{d^2u}{dy^2}(y) - R_c\lambda \frac{du}{dy}(y) = -1 \tag{A1}$$

The complementary function for Equation A1 is

$$u_c(y) = c_1 e^{R_c\lambda y} + c_2 \tag{A2}$$

Using the method of undetermined coefficients let us find a particular integral for Equation A1. We assume a particular solution of the form

$$u_p(y) = c_3 y \tag{A3}$$

which yields,

$$u_p(y) = \frac{y}{R_c\lambda} \tag{A4}$$

Application of the boundary conditions,

$$u(0) = 0,\ u(1) = 0 \tag{A5}$$

results in the solution for the fully developed velocity profile as,

$$u(y) = \frac{1}{R_c\lambda}\left[y - \frac{1 - e^{R_c\lambda y}}{1 - e^{R_c\lambda}}\right] \tag{A6}$$

It is easily shown by application of L'Hopital's rule that the limit of Equation A6 is,

$$\underset{R_c\lambda \to 0}{\text{Limit}} \; u(y) = \frac{1}{2}(y - y^2) \tag{A7}$$

which checks the ordinary channel flow solution without wall blowing. Profiles of the non-dimensionalized velocity as a function of the wall blowing parameter, $R_c\lambda$, are presented in Figure A1. Investigation of the effect of the wall blowing parameter on the fully developed velocity profile resulted in the selection of $R_c\lambda$ = 0.1, 1, 5, and 10 for further calculations.

The mean velocity, V_m, is defined as

$$V_m = \frac{1}{L}\int_o^L V_3(x_2)dx_2 = V_c \int_o^1 u(y)dy \tag{A8}$$

A dimensionless mean velocity is defined as

$$u_m = \frac{V_m}{V_c} \tag{A9}$$

which becomes

$$u_m = \frac{e^{R_c\lambda}(2-R_c\lambda) - R_c\lambda - 2}{2R_c{}^2\lambda^2\,(1 - e^{R_c\lambda})} \tag{A10}$$

A plot of the non-dimensionalized mean velocity as a function of the wall blowing parameter is shown in Figure A2, page 74.

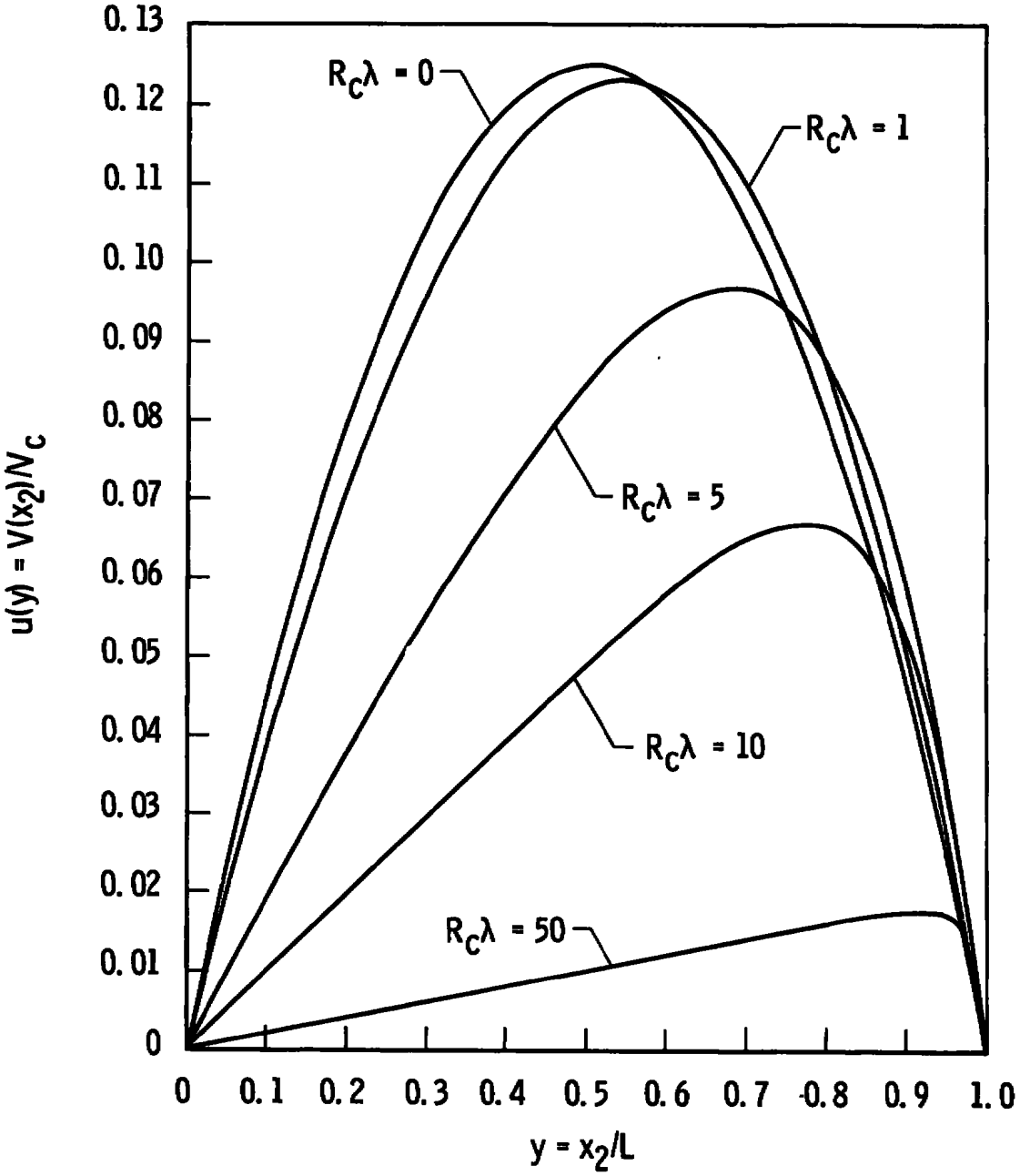

Fig. A1 Fully Developed Velocity Profiles as a Function of Wall Blowing Parameter

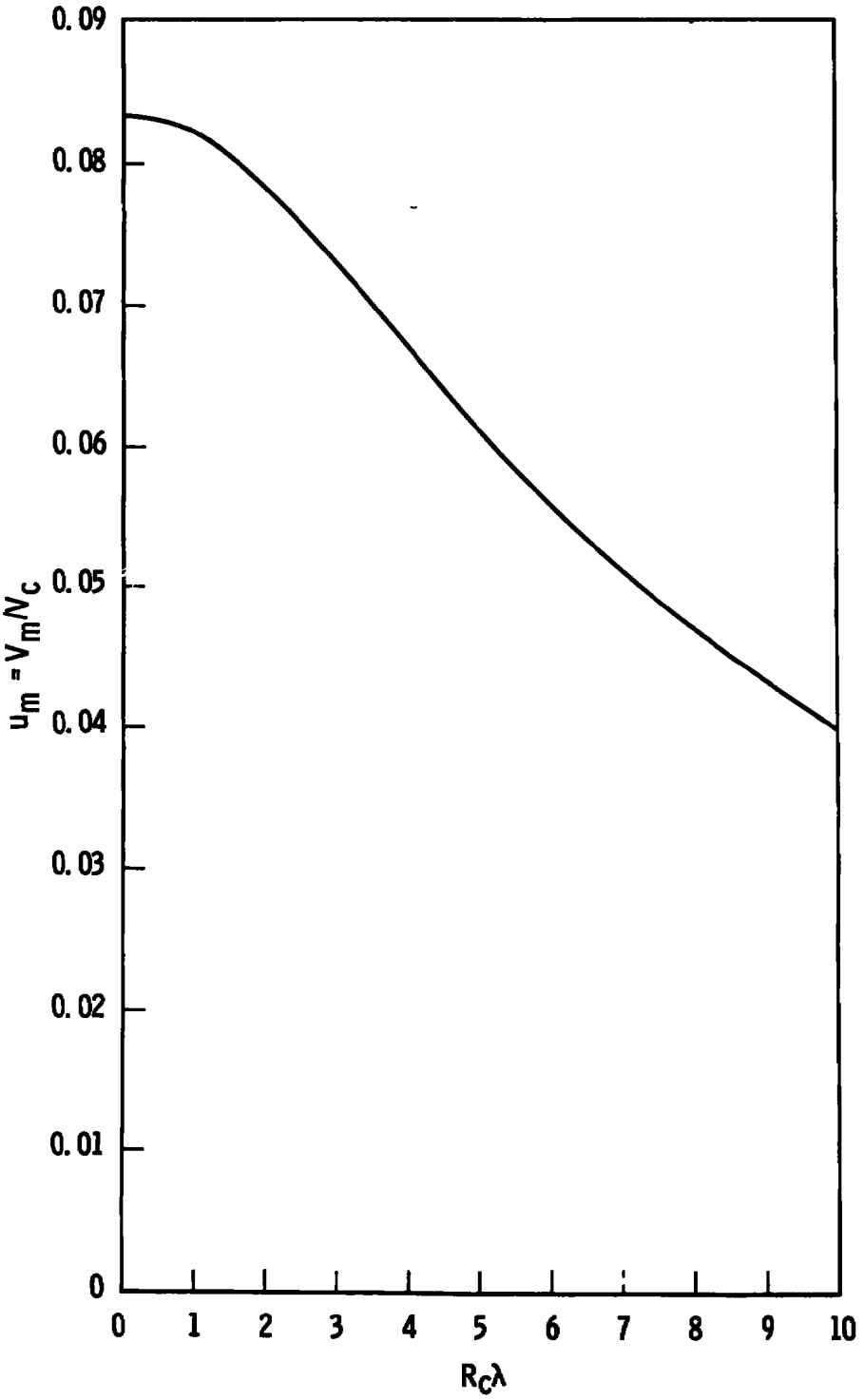

Fig. A2 Non-Dimensionalized Mean Velocity

APPENDIX B
SOLUTION FOR FULLY DEVELOPED DIMENSIONLESS TEMPERATURE PROFILE

The governing equation for the fully developed temperature profile is a non-homogeneous linear differential equation as follows from Equation 20,

$$\frac{d^2\theta_\infty}{dy^2}(y) - PrR_c\lambda \frac{d\theta_\infty}{dy}(y) = -PrEc\left[\frac{du}{dy}(y)\right]^2 \qquad (B1)$$

with boundary conditions

$$\theta_\infty(1) = 0 \quad , \quad \theta_\infty(0) = 0 \qquad (B2)$$

Since the analytic solution for the fully developed temperature profile is a very complicated expression, an extensive simplification in evaluation of the integral, Equation 49, is possible by using the G. B. Galerkin method to obtain a series solution for Equation B1. Defining a new function as

$$G_\infty(y) = e^{-\frac{1}{2}PrR_c\lambda y}\ \theta_\infty(y) \qquad (B3)$$

which is substituted into Equation B1 to yield,

$$\frac{d^2G_\infty}{dy^2}(y) - \frac{Pr^2R_c{}^2\lambda^2}{4} G_\infty(y) = -PREce^{-\frac{1}{2}PrR_c\lambda y}\left[\frac{du}{dy}(y)\right]^2 \qquad (B4)$$

Assume an approximate solution of Equation B4 as

$$G_\infty(y) = \sum_{i=1}^{M} D_i' \sin i\pi y \tag{B5}$$

Substitute Equation B5 into Equation B4 which gives,

$$\sum_{i=1}^{M} D_i' \left\{ -i^2\pi^2 \sin i\pi y - \frac{Pr^2 R_c^2 \lambda^2}{4} \sin i\pi y \right\} =$$

$$- PrEc\, e^{-\frac{1}{2}PrR_c\lambda} \left[\frac{du}{dy}(y)\right]^2 \tag{B6}$$

Following the method of B. G. Galerkin hence multiplying Equation B6 by $\phi_k(y) = \sin k\pi y$ and integrating over the range $0 \leq y \leq 1$,

$$\sum_{i=1}^{M} D_i' \left[-i^2\pi^2 - \frac{Pr^2 R_c^2 \lambda^2}{4} \right] I_1(k,i) = -PrEcI_2(k)$$

$$k = 1,2,3, \ldots. M \tag{B7}$$

where the integrals are given by:

$$I_1(k,i) = \int_0^1 \sin i\pi y \sin k\pi y\, dy = \frac{1}{2}\, \delta_{ik} \tag{B8}$$

$$I_2(k) = \int_o^1 e^{-\frac{1}{2}PrR_c\lambda y} \left[\frac{du}{dy}(y)\right]^2 \sin k\pi y \, dy =$$

$$\frac{4\pi}{R_c^2\lambda^2}\left\{\left[\frac{k}{Pr^2R_c^2\lambda^2+4k^2\pi^2}\right]\left[1 - e^{-\frac{1}{2}PrR_c\lambda}(-1)^k\right] + \left[\frac{2R_c\lambda}{1-e^{R_c\lambda}}\right]\left[\frac{k}{(2R_c\lambda-PrR_c\lambda)^2+4k^2\pi^2}\right]\left[1-e^{(R_c\lambda-\frac{1}{2}PrR_c\lambda)}(-1)^k\right] + \left[\frac{R_c^2\lambda^2}{(1-e^{R_c\lambda})^2}\right]\left[\frac{k}{(4R_c\lambda-PrR_c\lambda)^2+4k^2\pi^2}\right]\left[1-(-1)^k e^{(2R_c\lambda-\frac{1}{2}PrR_c\lambda)}\right]\right\} \quad (B9)$$

Equation B7 is a non-homogeneous system of linear equations which can be solved to determine the D_i''s. Since $I_1(k,l)$ is the Kronecker delta Equation B7 can be written as follows,

$$D_i' = \frac{-2PrEc\, I_2(i)}{\left[-i^2\pi^2 - \frac{Pr^2R_c^2\lambda^2}{4}\right]} \quad (B10)$$

If D_i' is redefined as,

$$D_i = \frac{-2I_2(i)}{\left[-i^2\pi^2 - \frac{Pr^2R_c^2\lambda^2}{4}\right]} \quad (B11)$$

then,

$$G_\infty(y) = PrEc \sum_{i=1}^{M} D_i \sin i\pi y \quad (B12)$$

From Equation B3 the fully developed dimensionless temperature profile becomes

$$\theta_\infty(y) = e^{\frac{1}{2}PrR_c\lambda y}\, G_\infty(y) =$$

$$PrEc\, e^{\frac{1}{2}PrR_c\lambda y} \sum_{i=1}^{M} D_i \sin i\pi y \qquad \text{(B13)}$$

The approximate solution for the present study was obtained by using twenty terms. M = 20, in the series solution.

DOCUMENT CONTROL DATA - R & D

(Security classification of title, body of abstract and indexing annotation must be entered when the overall report is classified)

1. ORIGINATING ACTIVITY *(Corporate author)*
Arnold Engineering Development Center
ARO, Inc., Operating Contractor
Arnold Air Force Station, Tennessee

2a. REPORT SECURITY CLASSIFICATION
UNCLASSIFIED

2b. GROUP
N/A

3. REPORT TITLE
TEMPERATURE DEVELOPMENT IN THE ENTRANCE REGION OF A PARALLEL PLATE CHANNEL WITH WALL BLOWING

4. DESCRIPTIVE NOTES *(Type of report and inclusive dates)*
December 1967 to April 1968 _ Final Report

5 AUTHOR(S) *(First name, middle initial, last name)*
James R. Blanks, ARO, Inc.

6. REPORT DATE	7a. TOTAL NO. OF PAGES	7b. NO. OF REFS
May 1969	88	17

8a. CONTRACT OR GRANT NO. F40600-69-C-0001

b. PROJECT NO. 876A

c. Program Element 65401F

d. Task G226

9a. ORIGINATOR'S REPORT NUMBER(S)
AEDC-TR-69-58

9b. OTHER REPORT NO(S) *(Any other numbers that may be assigned this report)*
N/A

10. DISTRIBUTION STATEMENT
This document has been approved for public release and sale; its distribution is unlimited.

11. SUPPLEMENTARY NOTES
Available in DDC.

12. SPONSORING MILITARY ACTIVITY
Arnold Engineering Development Center, Air Force Systems Command, Arnold AF Station, Tennessee 37389

13 ABSTRACT

The general mathematical problem of the thermal entrance region is formulated for a parallel plate channel by including the effects of viscous dissipation, axial conduction, and wall blowing. The associated eigenvalue problem is solved by the B. G. Galerkin method and the results are presented for constant wall temperature. It is shown that the particular method has distinct computational advantages over the classical form of solutions. The constant wall temperature case is investigated by employing the solutions of the eigenvalue problem, and it is concluded that the wall blowing parameter has considerable effect on the temperature development. The axial conduction term is also shown to have considerable effect on the temperature development for low values of Peclet number.

DD FORM 1 NOV 65 1473

14. KEY WORDS	LINK A		LINK B		LINK C	
	ROLE	WT	ROLE	WT	ROLE	WT
laminar flow						
viscous flow						
heat transmission						
steady flow						
heat transfer						
Nusselt number						